

Dynamic Modeling of a Solar Powered Thermal Energy Storage System for Cooking

TKP4580 - Chemical Engineering, Specialization Project

Mikal Rekdal

Supervisor: Prof. Johannes Jäschke

Co-supervisor: Prof. Ole Jørgen Nydal

Autumn 2019

Norwegian University of Science and Technology

Department of Chemical Engineering

Contents

Summary

1	Introduction	1
1.1	Motivation	1
1.2	Objectives	2
2	Theory	3
2.1	System Description	3
2.2	Assumptions	5
2.3	Tank 1	5
2.4	Tank 2	11
2.5	Cooking Pan	12
2.6	Food in Casserole	13
2.7	Tank 3	14
3	Methods	16
4	Results	19
4.1	Case 1: Heating of Storage Tank	19
4.2	Case 2: Cooking With Full Storage Tank	21
4.2.1	Comparison of Constant Flow and Temperature Controlled Flow	21
4.2.2	System Response with Temperature Control	21
4.3	Case 3: Cooking with Oil Circulation	24
4.4	Case 4: Heat Loss from Tank 2	25
5	Discussion	26
5.1	Method Evaluations	26
5.2	Discussion of Results	26
5.3	Parameter Estimation	28
5.4	Field Test Suggestions	30
5.5	Further Work	30
6	Conclusion	31
	Appendices	i
A	Additional Case Studies and Plots	i
A.1	Case 1c: Comparison of Heating Gradually Filling and Filled Tank	i
A.2	Case 2: Constant Hot Oil Flow Rate - Plots	i
B	Hand Calculations	iii
B.1	Rice Cooking Estimations	iii
B.2	Case 2: Average Experimental Heat Transfer	iii

C	MATLAB Codes	iv
C.1	Case 1a Simulation	iv
C.2	Liquid Level and Heat Transfer Area Calculation	vii
C.3	Case 2: Cooking with Temperature Control Simulation	viii
D	Simulation Parameters	xiii

List of Figures

2.1	Picture of the system assembled at the NTNU laboratory.	3
2.2	Schematic illustration of system's main components and streams	4
2.3	Mass and energy in- and outflows of tank 1.	5
2.4	End dimensions of a partially filled cylindrical tank	8
2.5	Heat loss transfer area dimensions for a partially filled tank	9
2.6	Mass and energy in- and outflows of tank 2.	11
2.7	Mass and energy in- and outflows of the oil bath in the cooking pan.	12
2.8	Energy in- and outflows of the water/food in the casserole.	14
2.9	Mass and energy in- and outflows of tank 3.	14
3.1	Illustration of case study 1 and 2	17
3.2	Illustration of case study 3 and 4	17
4.1	Left: Temperature in the full tank 2. Right: Heat input during heating of the full tank.	19
4.2	Left: Temperature in tank 2 during heating and gradual filling of an initially nearly empty tank 2. Right: Mass flow from tank 1 to 2 during the simulation.	20
4.3	Levels in tank 1 and 2, h_1 and h_2 , during heating and gradual filling of an initially nearly empty tank 2.	20
4.4	Temperatures in tank 2, cooking pan, water and tank 3 during heating and boiling of water.	21
4.5	Left: Liquid level in tank 2 during the heating and boiling with temperature control. Right: Mass flow rate from tank 2 to the cooking pan during the simulation.	22
4.6	Heat transfer values during heating and boiling of the water.	22
4.7	Time the system can operate if maintaining a boiling or simmering temperature.	24
4.8	Temperature profiles in all control volumes with cooking and recirculation of warm oil.	24
4.9	Volume fractions in tanks during cooking and circulation of warm oil.	25
4.10	Temperature of tank 2 with a varying volume fraction, F_2 . The lines of fractions 1.0 and 0.5 overlap.	25
5.1	Time required to heat a full tank 2 from 66 °C to 250 °C with a varying heat loss coefficient, U_2	29
5.2	Time water is maintained at boiling temperature with varying the heat loss factor for the cooking pot surface, UA_f	29
A.1	Left: Comparison of temperature profiles with an initially full or gradually filling tank. Right: Tank 2 volume fractions during the simulation	i

A.2 Left: Temperatures in tank 2, cooking pan, water and tank 3 with a constant mass flow of 0.001 kg/s through the pan. Right: Volume fraction of tank 2 during heating and boiling of water. ii

A.3 Left: Temperatures in tank 2, cooking pan, water and tank 3 with a constant mass flow of 0.0005 kg/s through the pan. Right: Volume fraction of tank 2 during heating and boiling of water. ii

List of Tables

2.1	System Parts of Figure 2.1	4
3.1	Variable Parameters for Case Studies	18
4.1	Cooking Time Results for Various \hat{m}_{2P} Values	21
4.2	Average Heat Transfers at Water Boiling Temperature	23
4.3	Time and Average Heating Output to Reach Water Boiling Temperature	23
D.1	Parameters Used in MATLAB Simulations	xiii

List of Symbols

- A_h Tank end area of section filled with liquid [m^2]. 8, 9
- A_p Casserole bottom area [m^2]. xiii, 13
- A_{tank} Tank surface area in contact with oil [m^2]. 9, 10, 12, 15
- A_t Cross-sectional area of thermostat opening [m^2]. 6–8
- A_v Cross-sectional area of manual valve opening [m^2]. xiii, 7
- A Full tank end area [m^2]. xiii, 8
- C_t Thermostat discharge coefficient [-]. xiii, 6, 7
- C_v Manual valve discharge coefficient [-]. xiii, 7
- C_p Heat capacity [J/kgK]. xiii, 10, 12–15
- F_{tot} Frictional terms [m^{-4}]. 7, 11
- F Filled volume fraction in tank [-]. i, 8, 17, 18, 21, 24, 25
- J Energy [J]. iii, 23
- L Tank length [m]. xiii, 9
- T_1 Temperature in tank 1 [K]. 10, 12
- T_2 Temperature in tank 2 [K]. 7, 12, 13, 17, 18, 26
- T_3 Temperature in tank 3 [K]. 10, 15
- T_F Temperature in control volume F [K]. 12–14
- T_P Temperature in control volume P [K]. 12, 13, 15
- T_R Room temperature [K]. 10, 12, 14, 15, 26
- T_f Thermostat control final temperature [K]. 7, 12
- T_s Thermostat control start temperature [K]. 7, 12
- UA_f Heat transfer factor [W/K]. 14, 28, 29, 31
- U Overall heat transfer coefficient [W/ m^2 K]. xiii, 10, 12, 15, 28–30
- V Full tank volume [m^3]. xiii, 8

$\Delta H_{vap,water}$ Vaporization enthalpy of water [J/kgK]. 14
 $\Delta P_{friction}$ Frictional pressure drop [Pa]. 6
 $\Delta P_{thermostat}$ Thermostatic valve pressure drop [Pa]. 6, 7
 ΔP_{valve} Manual valve pressure drop [Pa]. 6, 7
 \hat{Q}_{1R} Heat loss from tank 1 [W]. 5, 10
 \hat{Q}_{2R} Heat loss from tank 2 [W]. 11, 12, 23
 \hat{Q}_{3R} Heat loss from tank 3 [W]. 14, 15
 \hat{Q}_{FR} Heat loss from water in casserole [W]. 13, 14, 23
 \hat{Q}_{PF} Heat transferred from pan to water [W]. iii, 12–14, 22, 23, 27
 \hat{Q}_{PR} Heat loss from cooking pan [W]. 12–14, 23
 \hat{Q}_{PV} Solar powered heating input [W]. xiii, 11, 12, 18, 30
 \hat{Q} Heat flow [W]. 9, 10
 \hat{m}_{12} Mass flow from tank 1 to 2 [kg/s]. 5–7, 9, 11, 12, 18
 \hat{m}_{2P} Mass flow from tank 2 to cooking pan [kg/s]. 11, 13, 18, 21
 \hat{m}_{31} Mass flow from tank 3 to 1 [kg/s]. 5, 6, 10, 14, 15, 18
 \hat{m}_{P3} Mass flow from cooking pan to tank 3 [kg/s]. 11, 12, 14, 15
 \hat{m}_{pump} Manual pump mass flow [kg/s]. xiii, 6
 ρ Density [kg/m³]. xiii, 6–8, 11
 θ Central angle [-]. 8, 9
 g Acceleration of gravity [m/s²]. xiii, 6, 7, 11
 h_{12} Pipe height difference between tank 1 and 2 [m]. xiii, 6
 h_1 Liquid level height tank 1 [m]. 6–8, 11, 20
 h_{23} Pipe height difference between tank 2 and 3 [m]. xiii, 11
 h_2 Liquid level height tank 2 [m]. 6–8, 11, 20
 h_3 Liquid level height tank 3 [m]. 11
 h_{PF} Heat transfer coefficient [W/m²K]. xiii, 13

l Heat loss factor [-]. xiii, 13, 28

m Mass [kg]. 8, 10

r Tank radius [m]. xiii, 8, 9

x Opening fraction of thermostat valve [-]. 7, 8, 12

H Enthalpy [J/kgK]. 9, 10

m_1 Mass in tank 1 [kg]. 6, 10

m_2 Mass in tank 2 [kg]. 11, 12

m_3 Mass in tank 3 [kg]. 15

m_F Mass in casserole [kg]. 13, 14

m_P Mass in cooking pan [kg]. 13

Summary

A solar powered thermal energy storage system has been assembled at the Norwegian University of Science and Technology (NTNU) and in Tanzania. The system consists of three oil tanks that uses heated oil as a heat transfer medium to cook food. Its purpose is to provide a simple cooking system when excess renewable electricity is produced. The system could replace biomass stoves in developing areas, which produce toxic fumes. In this project, a dynamic model of the system was established. The model was used to simulate and evaluate the thermal storage properties and cooking capacity of the system. All simulations were performed in MATLAB, in a series of case studies to compare the model's behavior to that of the physical system.

Like previous field tests, the simulations demonstrate sufficient energy output to cook food. A full tank of hot oil keeps 10 L of water boiling for 1.18 hours. This capacity corresponds to cooking approximately 80 portions of rice. The largest uncertainties in the model are associated with heat losses from the system. These losses largely depend on the amount of insulation used in the finalized physical design. Additional field tests could be conducted to obtain more certain estimates of the heat transfer parameters.

1 Introduction

The energy demand is increasing with a growing world population. According to British Petroleum's annual review of world energy, the global primary energy consumption grew by 2.9 % in 2018. In the same year, carbon emissions from energy production saw its highest growth rate since 2010/2011. Although the renewable power supply grew by 14.5 %, it only accounted for 9.3 % of the total power generation. The report emphasises that a faster transition to renewable energy is required to reach the Paris climate goals [1]. However, this transition poses challenges in providing a reliable energy supply to a growing population.

Solar and wind power are the fastest growing renewable sources globally. In many regions of the world, solar and wind power are rapidly emerging technologies [1]. The major challenge with solar and wind are their variable energy supply. This is especially challenging in rural and remote areas that are not connected to other power sources. One solution is to store the power generated when the supply is higher than the demand. This buffer of stored energy would allow for utilization of the excess energy at times when power is not generated [2].

There are a number of techniques for storing produced renewable electricity. Their main purpose is to increase the reliability and robustness of the power supply. The technologies store electrical energy in other electrical, thermal, chemical, mechanical or electrochemical forms. For this project, thermal energy storage is of particular interest. Typically, an electrical resistor is used to heat up a stored medium such as hot water, molten salts or other materials. The heat can then be utilized in a heat engine to produce electricity. Another option is to use the medium directly as the heating source in a heat exchanger [3].

Rural areas of developing countries are good candidates for implementing simple energy storage systems. Off-grid communities would be provided with access to clean energy with improved reliability by the opportunity of storing the energy when excess power is produced. These areas often depend on firewood for cooking. In Central, East, Southern and West Africa, cooking accounts for nearly 80% of residential energy consumption. The use of traditional biomass stoves pose both health and economic issues. Approximately 600 000 people die each year in these regions from exposure to toxic fumes [4]. In addition, economic implications include hours spent on collecting biomass and inefficient cooking. Replacing these stoves with electrical appliances or emission free solar cookers could therefore have significant health and economic benefits.

1.1 Motivation

The Department of Energy and Process Engineering at NTNU have developed and assembled a thermal energy storage system at their laboratories. The system uses excess solar

power to heat palm oil that can be used as a heat source for cooking. The motivation behind the system is to provide a simple, low-maintenance cooking application for rural areas. An equivalent system has been set up in Arusha, Tanzania and was field tested in the spring of 2019 as part of a master project at NTNU [5]. In this project, a dynamic model of the system has been developed. The purpose of the mathematical simulation is to evaluate the system's performance at various conditions. In the spring, the model will be further developed. Then, the operation of the system will be optimized in terms of energy efficiency and to simulate scale-up possibilities for implementation in larger communities.

1.2 Objectives

The main purpose of this project was to develop a realistic dynamic model of the assembled thermal energy storage system. Thus, the following objectives were established

1. Develop a model based on physical principles, with known and estimated parameters of the system.
2. Create case studies and run simulations to investigate the system behavior.
3. Compare the model performance to available experimental data.

2 Theory

In the following section, the physical system subject to modeling is described. Then, the derivation of the model and relevant theory is discussed.

2.1 System Description

Figure 2.1 below shows the system at the NTNU laboratory, with a description of the components in table 2.1. A flow chart of the system follows in figure 2.2 to illustrate and describe the key components more clearly.



Figure 2.1: Picture of the system assembled at the NTNU laboratory. The equivalent system in Arusha contains a larger cooker (8) and no frying pan (9). The picture and table 2.1 below are retrieved from reference [5].

Table 2.1: System Parts of Figure 2.1

Number	Part
1	Tank 1
2	Tank 2 (storage)
3	Tank 3
4	PicoLogger
5	Power supply cables to heating elements
6	Hand pump
7	Hose to flush pan
8	Cooker
9	Frying pan
10	Tray for spilling
11	Valve to tank 1
12	Valve to frying pan

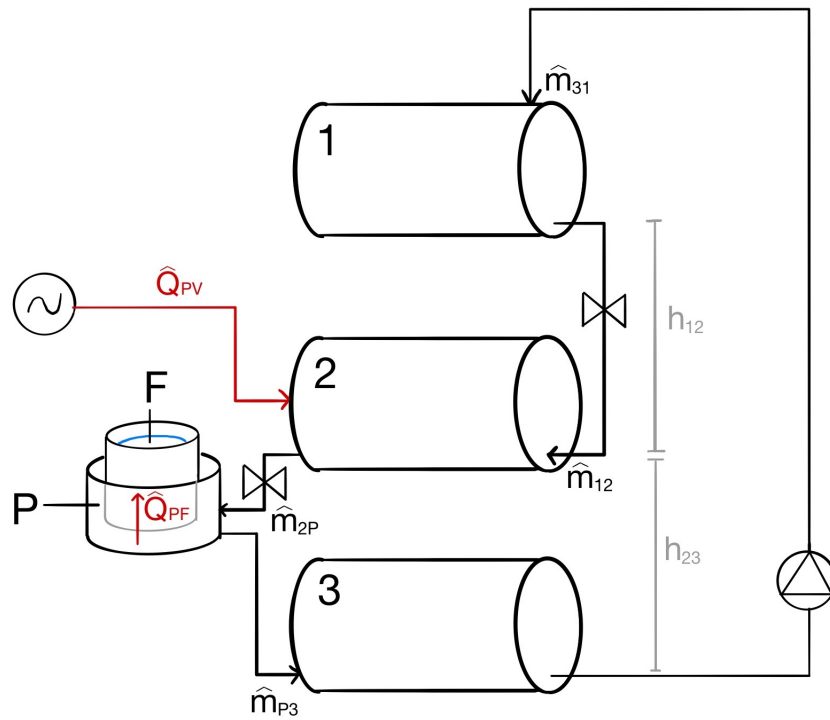


Figure 2.2: Schematic illustration of the system's main components and streams. Red arrows indicate heat transfer while black arrows are mass transfers. A heat loss from each control volume to the environment has been modeled but not depicted here.

The system consists of three oil tanks, denoted as control volume 1, 2 and 3 in figure 2.2. The flow of oil from top to bottom is gravity driven. Electrical heating elements powered by solar panels are placed in tank 2 to heat up the oil. Two valves are installed to adjust the

flow from tank 1 to tank 2. A thermostatic valve can be opened to control the maximum temperature in tank 2, or another valve can adjust the flow rate manually. In this project, only a cooker was considered for preparing food, consistent with the system setup in Arusha. Therefore, the frying pan will not be discussed further. A third valve which is manually operated, is installed between tank 2 and the cooker. When opened, the hot oil flows through the cooking pan, denoted control volume P, where a casserole containing water is placed. The casserole is heated by the hot oil flowing around the container, which then heats the water/food inside, named control volume F. The oil exits the cooking pan and accumulates in tank 3. A manual pump is installed to pump the oil back up to tank 1. In the following subsections, the model for each control volume is discussed.

2.2 Assumptions

In establishing a model of the system, the following assumptions were made

1. The heat capacity of the oil and the water is constant.
2. The system's cooking time capacity is the time water can be kept at its boiling point.
3. The oil is well mixed in all flows and control volumes, giving a uniform temperature.
4. The water is well mixed in the casserole with a uniform temperature.
5. Only tank area in direct contact with oil has significant heat loss to the environment.
6. Pipes are well isolated, resulting in negligible heat loss.

Additional assumptions have been made when deriving the model equations for each control volume. These are addressed in subsections where they are applicable.

2.3 Tank 1

For tank 1, three flows are considered associated with the control volume. There is the mass and enthalpy inflow from tank 3 to 1, \hat{m}_{31} , the outflow from tank 1 to tank 2, \hat{m}_{12} , and the heat loss from tank 1 to the room, \hat{Q}_{1R} . The flows are marked in figure 2.3 below

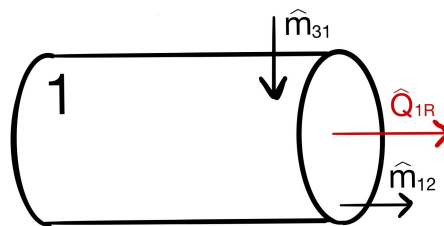


Figure 2.3: Mass and energy in- and outflows of tank 1.

Mass Balance

The accumulation of mass in the control volume, \dot{m}_1 , can be described as the difference between in- and outflows, here \hat{m}_{31} and \hat{m}_{12} respectively

$$\dot{m}_1 = \hat{m}_{31} - \hat{m}_{12} \quad (2.1)$$

The inflow is set by the pumping rate \hat{m}_{pump} , which is an input to the system by operating the manual hand pump

$$\hat{m}_{31} = \hat{m}_{pump} \quad (2.2)$$

The mass flow from tank 1 to 2 is gravity driven. The flow passes through the pipe, manual valve and the thermostatic valve from the first tank to the second. The manually controlled valve is considered to be fully open. Thus, the opening of the thermostatic valve at the entrance of tank 2 limits the flow. For calculating the flow, it was assumed that there is a steady state balance between the pressure difference of the tanks and the friction loss. In other words,

$$\rho g h_1 + h_{12} - h_2 = \Delta P_{friction} \quad (2.3)$$

where h_1 and h_2 are the liquid levels in tank 1 and 2 and g is the standard acceleration of gravity. h_{12} is the height difference between the outlet of tank 1 and inlet of tank 2, depicted in figure 2.2. Due to the short length of the pipes, it was assumed that this pipe friction contribution is negligible. The friction loss, $\Delta P_{friction}$, is then due to flow through the thermostat, $\Delta P_{thermostat}$, and the manually operated valve, ΔP_{valve} . Rewriting of equation 2.3 gives

$$\rho g \Delta h_1 = \Delta P_{valve} + \Delta P_{thermostat} \quad (2.4)$$

Where

$$\Delta h_1 = h_1 + h_{12} - h_2 \quad (2.5)$$

The flow across the thermostat is modeled by a typical valve equation

$$\hat{m}_{12} = C_t A_t \sqrt{2\rho \Delta P_{thermostat}} \quad (2.6)$$

with C_t being the discharge coefficient and A_t the area of the thermostat opening.

Rearranging equation 2.6 and solving for pressure drop across the thermostat gives

$$\Delta P_{thermostat} = \frac{\hat{m}_{12}^2}{(C_t A_t)^2 2\rho} \quad (2.7)$$

The equivalent expression is used for pressure drop across the manual valve

$$\Delta P_{valve} = \frac{\hat{m}_{12}^2}{(C_v A_v)^2 2\rho} \quad (2.8)$$

Thus, the following relation is established combining equation 2.4 and equations 2.7-2.8

$$\rho g \Delta h_1 = \frac{\hat{m}_{12}^2}{2\rho} \left(\frac{1}{(C_t A_t)^2} + \frac{1}{(C_v A_v)^2} \right) \quad (2.9)$$

Collecting the friction terms

$$F_{tot} = \frac{1}{(C_t A_t)^2} + \frac{1}{(C_v A_v)^2} \quad (2.10)$$

Finally, the mass flow then becomes

$$\hat{m}_{12} = \rho \sqrt{\frac{2g\Delta h_1}{F_{tot}}} \quad (2.11)$$

Three variables are still missing before the mass flow in equation 2.11 can be calculated. These are A_t , h_1 and h_2 .

Thermostat Control

The mass flow \hat{m}_{12} is controlled by the opening fraction of the thermostat hole, as seen from equation 2.11 and 2.10. The thermostat opening fraction was assumed to be a linear function of temperature. The valve is fully closed until a certain temperature, T_s , is reached. To limit the temperature in T_2 , the valve is fully open at a maximum temperature, T_f . The fraction of the area opened, x , is

$$x = \begin{cases} 0 & \text{if } T_2 \leq T_s \\ \frac{T_2 - T_s}{T_f - T_s} & \text{if } T_s < T_2 \leq T_f \\ 1 & \text{if } T_2 > T_f \end{cases} \quad (2.12)$$

The cross-sectional opening area of the thermostat hole, A_t , is then

$$A_t = \pi r^2 x \quad (2.13)$$

Liquid Level and Heat Transfer Area

Finally, h_1 and h_2 can be found using geometric arguments. Beginning with the volume fraction of the tank occupied, F , calculated as

$$F = \frac{m}{\rho V} \quad (2.14)$$

with ρ being the density of the liquid, m the mass in tank 1 and V the volume of a full tank.

The tank end area of the liquid section, A_h , is a fraction of the total tank end area, expressed as

$$A_h = F\pi r^2 \quad (2.15)$$

Another expression for A_h can be found using the central angle, θ , illustrated below in figure 2.4

$$A_h = \frac{1}{2}r^2(\theta - \sin(\theta)) \quad (2.16)$$

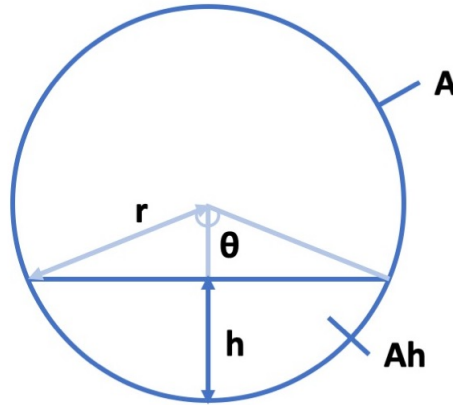


Figure 2.4: End dimensions of a partially filled cylindrical tank. A is the total area of the tank end, while A_h is the area of the tank end up to the filled liquid level h .

Combining equation 2.15 and equation 2.16, the following expression is obtained

$$\theta - \sin(\theta) = 2\pi F \quad (2.17)$$

which can be used to solve θ implicitly.

Then, the level in the tank, h , can be calculated by the radius of the tank, r , and θ as follows

$$h = r(1 - \cos(\frac{\theta}{2})) \quad (2.18)$$

The liquid level height of tank 2 is calculated using the same geometric arguments. Now, the mass transport \hat{m}_{12} is only expressed in known variables and can be calculated.

Lastly, the surface area of the tank in contact with the oil can be found. As mentioned, this is the area assumed to account for heat loss to the environment. The total contact area, A_{tank} , is the sum of A_h on both ends of the tank, and the product of the arc length ($r\theta$) and length of the tank, L , shown in figure 2.5 below

$$A_{tank} = 2A_h + r \theta L \quad (2.19)$$

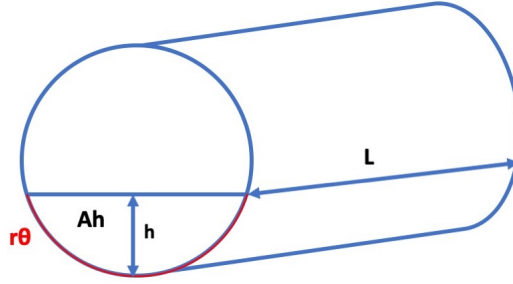


Figure 2.5: Heat loss transfer area dimensions for a partially filled tank. The oil contact surface area consists of the two tank ends, A_h , and the bottom area up to the liquid level, $r \theta L$.

Energy Balance

With the mass flows fully described, it is possible to develop the energy balance and temperature of tank 1. The general enthalpy balance for the control volume, assuming negligible pressure-volume work and shaft work, can be described by

$$\dot{H} = \sum \hat{H}_{in} - \sum \hat{H}_{out} + \hat{Q}_{net} \quad (2.20)$$

\dot{H} is the change in enthalpy with respect to time, \hat{H}_{in} and \hat{H}_{out} are the enthalpy flows in and out of the control volume and \hat{Q}_{net} is heat added through the wall. [6]

The enthalpy, H , is described by

$$H(T) = H(T_{ref}) + m \int_{T_{ref}}^{T} Cp(T) dT \quad (2.21)$$

where Cp is the heat capacity of the substance and $H(T_{ref})$ is the enthalpy at the reference temperature, T_{ref} . To evaluate the change in temperature in control volume i , \dot{T}_i , the enthalpy expression can be expanded

$$\dot{H}_i = \frac{d}{dt}(m_i Cp T_i) = \hat{m}_{in} Cp T_{in} - \hat{m}_{out} Cp T_{out} + \hat{Q}_{net} \quad (2.22)$$

$$Cp(\dot{m}_i T_i + \dot{T}_i m_i) = \hat{m}_{in} Cp T_{in} - \hat{m}_{out} Cp T_{out} + \hat{Q}_{net} \quad (2.23)$$

Here, $T_{out} = T_i$ and $\dot{m}_i = \hat{m}_{in} - \hat{m}_{out}$ so the temperature change is expressed by

$$\dot{T}_i = \frac{1}{m_i} (\hat{m}_{in} (T_{in} - T_i) + \frac{\hat{Q}_{net}}{Cp}) \quad (2.24)$$

For tank 1, the only heat transfer considered is heat loss from the tank surface to the room, \hat{Q}_{1R} . Thus, the following expression is found for tank 1

$$\dot{T}_1 = \frac{1}{m_1} (\hat{m}_{31} (T_3 - T_1) - \frac{\hat{Q}_{1R}}{Cp_{oil}}) \quad (2.25)$$

Heat Transfer

It was assumed that the convective heat loss \hat{Q}_{1R} follows Newton's law of cooling. The law states that the rate of heat loss is proportional to the difference in temperature between the body and its surroundings [7]

$$\hat{Q}_{1R} = U A_{tank} (T_1 - T_R) \quad (2.26)$$

where U is the heat transfer coefficient, assumed to be independent of temperature and T_R is the room temperature.

2.4 Tank 2

In tank 2, two mass streams are considered. These are the inflow from tank 1, \hat{m}_{12} , and the outflow to the cooking plate, \hat{m}_{2P} . Additionally, two heat transfers are considered. These are the input of the heating elements, \hat{Q}_{PV} and heat loss to the room, \hat{Q}_{2R} . All four flows are indicated in figure 2.6

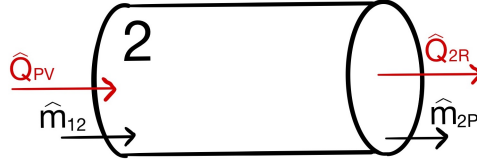


Figure 2.6: Mass and energy in- and outflows of tank 2.

The differential mass balance for tank 2 is

$$\dot{m}_2 = \hat{m}_{12} - \hat{m}_{2P} \quad (2.27)$$

\hat{m}_{12} is already expressed by equation 2.11, while \hat{m}_{2P} must be derived. The volume of control volume P is small compared to the three tanks. It was assumed to contain a constant mass, and that the flow quickly reached steady state. This means that the mass flow into P, \hat{m}_{2P} is equal to the outflow of P, \hat{m}_{P3}

$$\hat{m}_{2P} = \hat{m}_{P3} \quad (2.28)$$

Then, the mass flow \hat{m}_{2P} follows the pattern of equation 2.11. Using the level difference between tank 2 and tank 3

$$\hat{m}_{2P} = \rho \sqrt{\frac{2g\Delta h_2}{F_{tot}}} \quad (2.29)$$

Where

$$\Delta h_2 = h_2 + h_{23} - h_3 \quad (2.30)$$

with h_{23} being the height between the outlet of tank 2 and inlet of tank 3. h_2 is calculated in the same way as h_1 , by the derivation from equation 2.14 - 2.18.

In the current physical system, the valve for mass flow from tank 2 to the plate is manually controlled. However, it was of interest to see the response of the system by adding a thermostat valve that adjusts its opening fraction linearly like the thermostatic valve from tank 1 to 2. For \hat{m}_{2P} , the valve should be fully open initially and gradually close to limit

the heat flow as the temperature reaches its desired set point

$$x = \begin{cases} 1 & \text{if } T_P \leq T_s \\ 1 - \frac{T_P - T_s}{T_f - T_s} & \text{if } T_s < T_P \leq T_f \\ 0 & \text{if } T_P > T_f \end{cases} \quad (2.31)$$

The expression for the energy balance is quite similar as for tank 1. A heat loss from tank 2 to the room, \hat{Q}_{2R} , is also considered here. In addition, tank 2 has a heating input, \hat{Q}_{PV}

$$\dot{T}_2 = \frac{1}{m_2}(\hat{m}_{12}(T_1 - T_2) + \hat{Q}_{PV} - \frac{\hat{Q}_{2R}}{Cp_{oil}}) \quad (2.32)$$

\hat{Q}_{PV} is the delivered effect of the heating elements powered by solar panels. The heat loss to the room is also here assumed be significant for tank surface area in contact with the oil, giving

$$\hat{Q}_{2R} = U_2 A_{tank}(T_2 - T_R) \quad (2.33)$$

A different heat transfer coefficient value was used for tank 2 compared to 1 and 3 due to more insulation around this tank in the physical system.

2.5 Cooking Pan

In this model, a cooking pan is used for preparing food, consistent with the system in Arusha. Oil flows from tank 2 to the pan, which is a container of hot oil. The oil exits from the other side of the pan in mass stream \hat{m}_{P3} . Two heat transfers are associated with the control volume of oil, as shown in figure 2.7. These are a heat loss to the room, \hat{Q}_{PR} , and heat utilized to cook food, \hat{Q}_{PF} .

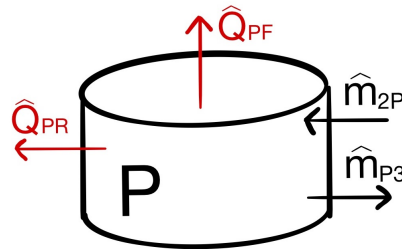


Figure 2.7: Mass and energy in- and outflows of the oil bath in the cooking pan.

Due to the assumption of steady state flow as stated in equation 2.28, the mass is constant

in the pan

$$\dot{m}_P = 0 \quad (2.34)$$

The expression for the temperature is then

$$\dot{T}_P = \frac{1}{m_P}(\hat{m}_{2P}(T_2 - T_P) - \frac{\hat{Q}_{PF}}{C_{p_{oil}}} - \frac{\hat{Q}_{PR}}{C_{p_{oil}}}) \quad (2.35)$$

For \hat{Q}_{PF} , it is assumed that an overall heat transfer coefficient can be found for the heat transfer through the metal casserole to the water. It is also assumed that only the bottom area of the casserole, A_p is submerged in oil and therefore the significant heat transfer area. The heat transferred from the hot oil to the water is then

$$\hat{Q}_{PF} = h_{PF}A_p(T_P - T_F) \quad (2.36)$$

with h_{PF} being the heat transfer coefficient through the casserole. The heat loss directly from the oil in the cooking pan to the room, \hat{Q}_{PR} , depends on various factors. One factor is the insulation efficiency of the container of the oil. Another is the amount of oil exposed directly to air, depending on the submerged casserole's size. Due to numerous uncertainties, a simple estimate of the heat loss was used. It was assumed that the heat loss was proportional to the heat transfer to the cooking casserole

$$\hat{Q}_{PR} = l\hat{Q}_{PF} \quad (2.37)$$

where l is the proportional heat loss factor.

2.6 Food in Casserole

Only the mass of water is considered in evaluating the enthalpy and temperature in the casserole. The addition of food, for instance rice, is assumed to have negligible effect on the mass and heat capacity in control volume F. Thus, the cooking time capacity was equivalent to time water is kept at boiling point. The casserole is likely to have a lid on to limit heat loss to the environment. The mass inside the casserole is then constant, without water evaporation

$$\dot{m}_F = 0 \quad (2.38)$$

For control volume F, shown in figure 2.8, the two flows to consider are therefore the heat loss to the room, \hat{Q}_{FR} , and the heat transfer from the pan, \hat{Q}_{PF}

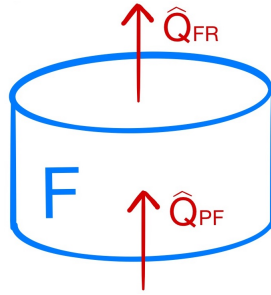


Figure 2.8: Energy in- and outflows of the water/food in the casserole.

For the water, two expressions have been implemented. When heating the water, the following energy balance was used

$$\dot{T}_F = \frac{1}{m_F C_{p_{water}}} (\hat{Q}_{PF} - \hat{Q}_{FR}) \quad (2.39)$$

As the water reaches boiling temperature, the additional energy supplied contributes to vaporizing the water

$$\dot{T}_F = \frac{1}{m_F \Delta H_{vap,water}} (\hat{Q}_{PF} - \hat{Q}_{FR}) \quad (2.40)$$

Like \hat{Q}_{PR} , the heat loss from the water to the room, \hat{Q}_{FR} , depends on numerous factors such as the size and material of the casserole. Therefore, a simple estimated heat transfer factor was introduced, UA_f , as a substitute for the overall heat transfer coefficient and transfer area

$$\hat{Q}_{FR} = UA_f (T_F - T_R) \quad (2.41)$$

2.7 Tank 3

Tank 3 also has a heat loss to the room, \hat{Q}_{3R} , as well as the in and out flows \hat{m}_{P3} and \hat{m}_{31} , shown in figure 2.9

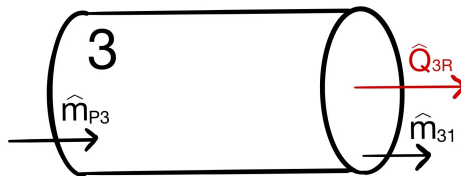


Figure 2.9: Mass and energy in- and outflows of tank 3.

The accumulation of m_3 is described by the in and out flows of discussed in equations 2.2 and 2.28

$$\dot{m}_3 = \hat{m}_{P3} - \hat{m}_{31} \quad (2.42)$$

Giving the following change in temperature

$$\dot{T}_3 = \frac{1}{m_3} (\hat{m}_{P3}(T_P - T_3) - \frac{\hat{Q}_{3R}}{C_{p_{oil}}}) \quad (2.43)$$

Like the other tanks, an equivalent heat loss expression has been established

$$\hat{Q}_{3R} = U A_{tank} (T_3 - T_R) \quad (2.44)$$

3 Methods

MATLAB scripts with some code were provided from the co-supervisor as a starting point for the model. All simulations were performed in MATLAB R2017b on a Macbook Air 2013 unless otherwise stated. The MATLAB codes developed can be found in appendix C.

A series of case studies were developed for various conditions. For all of the studies, the following general procedure in MATLAB was followed:

1. Initialization of the system parameters and definition of initial values. Determination of parameter values is described in appendix D.
2. Calculation of dynamic tank properties such as the liquid level and heat transfer area performed in a separate function.
3. Numerical solving of the differential equations for a constant time step.
4. Integration of the differential equations by Euler's method to compute the new system states.
5. Repetition of the three previous steps until a certain condition was met. Examples of conditions were reaching a maximum temperature in tank 2 or a predefined simulation time.
6. Plotting of selected system states of interest.

The case studies were based on the following simple operating procedure for the system. The oil is heated up in tank 2 in the morning to a certain temperature before shutting off the heating elements. Then, the oil flow to the cooking pan is initiated to heat up and boil water. As the level in tank 2 becomes low, oil is pumped back from tank 3 to tank 1 to utilize remaining heat energy in the system. If cooking is completed before sunset, any excess solar power can be stored by reheating oil in tank 2. Then, less time is required to heat up tank 2 in the morning to start cooking again.

This procedure is the basis for the development of the following case studies, illustrated in figures 3.1 and 3.2:

1. Time required to heat up tank 2, either starting with a full tank 2 or gradually filling the tank with oil from tank 1.
2. Cooking capacity of tank 2 filled with hot oil when emptied once.
3. Cooking capacity of tank 2 filled with hot oil when oil is pumped back from tank 3 to tank 1 to utilize remaining heat energy.
4. Temperature profile of tank 2 overnight for different filling fractions of oil.

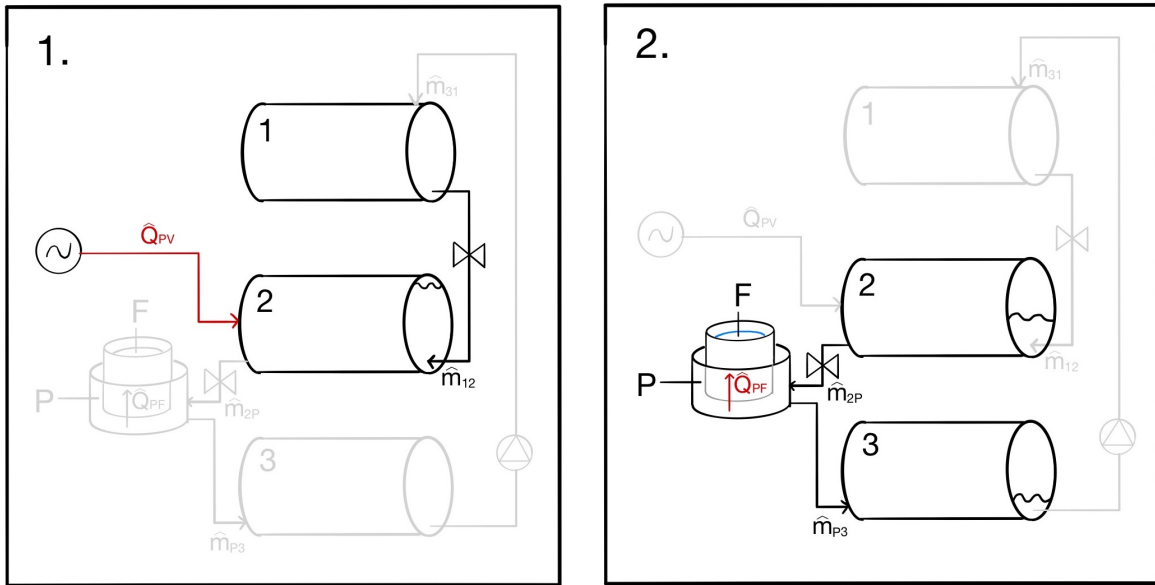


Figure 3.1: Illustration of case study 1 and 2. The active components under operation are highlighted. In case 1, the heating input and contents of tank 1 and 2 are of interest. In case 2, cooking is implemented by emptying tank 2, with the four lower control volumes being active components.

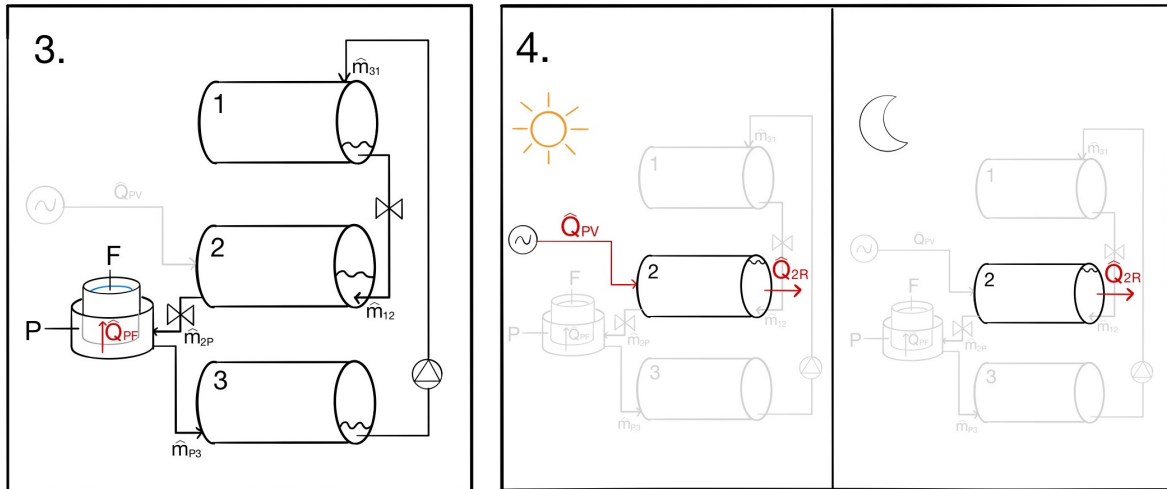


Figure 3.2: Illustration of case study 3 and 4. In case 3, all five control volumes are active components, with circulation of the oil from tank 3 to tank 1. In case 4, solar power heats a full tank 2 during daytime. At night, heat is lost from the tank.

Table 3.1 below reports the values used for variable conditions in the simulations.¹ These

¹TC indicates that the thermostatic valve was used to adjust the flow rate. For case 2, three different flow rates were tested separately. In case 3, the flow rates changed during the simulation. The second subscript of 0 for $T_{2,0}$, $F_{1,0}$ and $F_{2,0}$ indicate initial values at start time.

conditions were set to match previous field tests where an equivalent physical test has been performed.

Table 3.1: Variable Parameters for Case Studies

Case	$T_{2,0} [^{\circ}C]$	\hat{Q}_{PV} [W]	\hat{m}_{12} [kg/s]	\hat{m}_{2P} [kg/s]	\hat{m}_{31} [kg/s]	$F_{1,0}$ [-]	$F_{2,0}$ [-]
1a	66	1000	0	0	0	0	0.99
1b	25	1000	TC	0	0	0.90	0.05
2	250	0	0	0.01/0.005/TC	0	0	0.95
3	250	0	TC/0.001	0/0.001	0/0.001	0.05	0.95
4	220	0	0	0	0	0	0.125 - 1.0

4 Results

For improved readability, the conditions of each case study are largely described qualitatively below. The reader is encouraged to refer to table 3.1 or the attached MATLAB scripts for remaining quantitative conditions. All references made to field tests are experiments described in the thesis by Thaule et.al. [5].

4.1 Case 1: Heating of Storage Tank

The purpose of case 1 was to check that the temperature in tank 2 increased as heat was added to the system. Test 1b investigated the response of the system when thermostat control was implemented.

1a: Heating of Filled Storage Tank

The first simulation heated a full tank 2 from 66 °C to 250 °C with a constant heating input of 1000 W. A similar field test was performed for the system in Arusha, allowing for comparison of the data. The input and response are plotted in figure 4.1. It took 4.03 hours to heat the full tank to 250 °C.

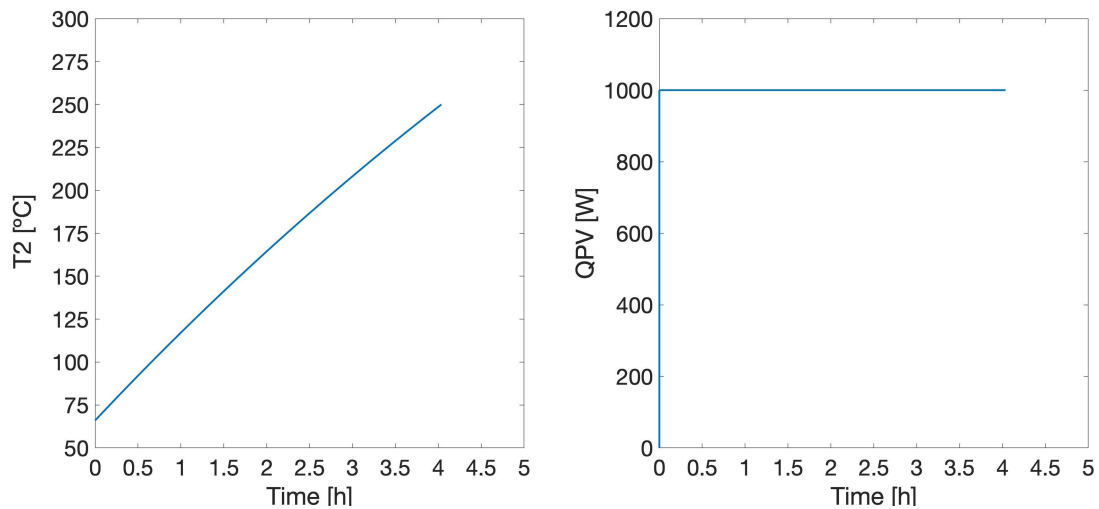


Figure 4.1: Left: Temperature in the full tank 2. Right: Heat input during heating of the full tank.

1b: Heating of Gradually Filling Storage Tank

Then, a simulation was performed to check that the thermostat control model for tank 2 was functioning. A nearly empty tank 2 was heated with an input of 1000 W. As the temperature reached 200 °C, the valve from tank 1 to tank 2 was opened. The flow was

regulated to keep the temperature in tank 2 below 250 °C, with oil from tank 1 at 25 °C. The simulation ran until the volume fraction of tank 2 was 0.9.

The temperature in tank 2 and mass flow from tank 1 to 2 is plotted in figure 4.2 below.

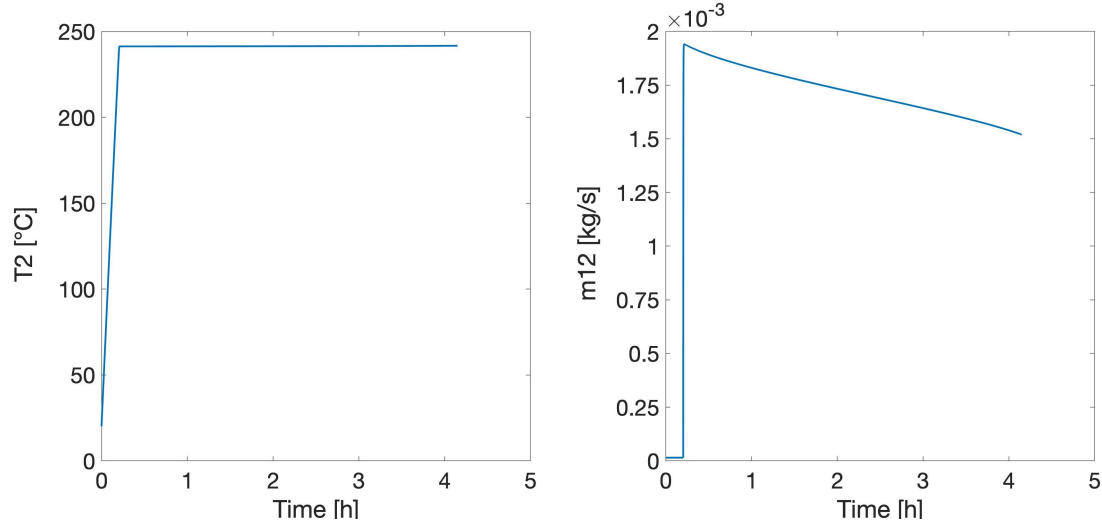


Figure 4.2: Left: Temperature in tank 2 during heating and gradual filling of an initially nearly empty tank 2. Right: Mass flow from tank 1 to 2 during the simulation.

It took 4.15 hours to heat the tank. The temperature of the tank is maintained between 241.3 and 241.7 °C throughout the heating. A plot of the liquid level in tank 1 and 2 is given in figure 4.3. After 12 minutes, the level in tank 2 starts to increase as the thermostat hole opens and cold oil flows from tank 1.

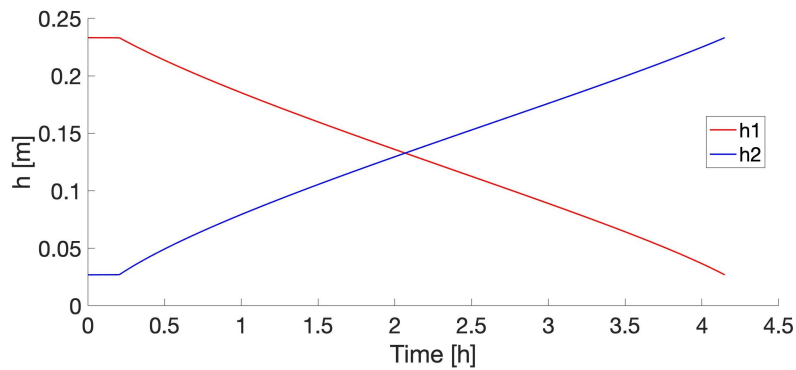


Figure 4.3: Levels in tank 1 and 2, h_1 and h_2 , during heating and gradual filling of an initially nearly empty tank 2.

A comparison of the heating time required with and without temperature control was also performed. The study can be found in appendix A.1.

4.2 Case 2: Cooking With Full Storage Tank

4.2.1 Comparison of Constant Flow and Temperature Controlled Flow

After heating the oil, it was of interest to see how long a full tank of hot oil could keep water boiling without additional solar input. Tank 2's initial temperature was 250 °C and 10 L of water was boiled. Two tests were run with a constant mass flow rate of 0.01 kg/s and 0.005 kg/s through the pan, \hat{m}_{2P} , respectively. The temperature profiles are found in appendix A.2. A third test was performed using thermostat control to regulate the temperature of the cooking plate. The plate was controlled to maintain a temperature of 104.5 °C, which stabilized the water temperature at 100.0 °C. All three simulations were ended when F_2 reached 0.05 and the results are reported in table 4.1

Table 4.1: Cooking Time Results for Various \hat{m}_{2P} Values

Mass Flow [kg/s]	Time to Boil [h]	Simulation End Time [h]	Cooking Time Capacity [h]
0.01	0.293	0.719	0.426
0.005	0.682	1.438	0.756
TC ²	0.276	1.454	1.178

4.2.2 System Response with Temperature Control

The system behavior using the thermostatic valve was further investigated in the subsequent plots. In figure 4.4, the temperatures in the four lower control volumes are plotted during the simulation.

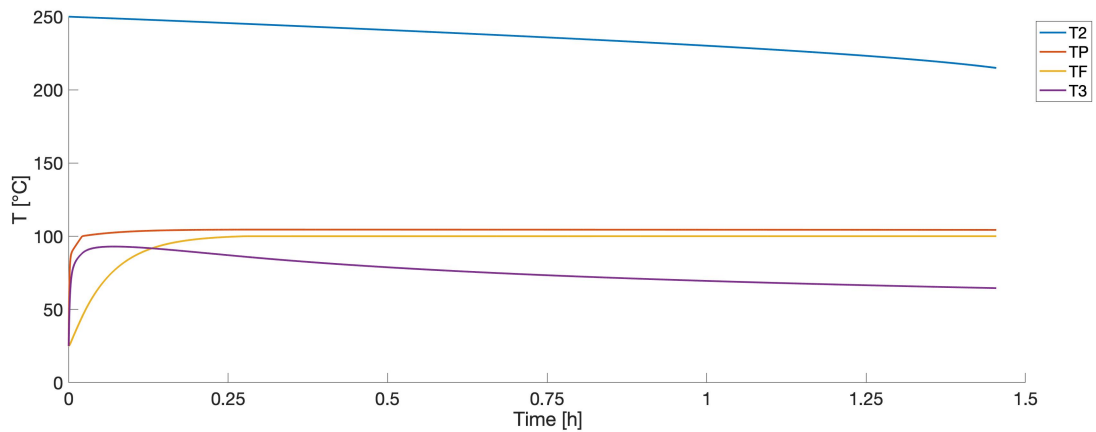


Figure 4.4: Temperatures in tank 2, cooking pan, water and tank 3 during heating and boiling of water. Temperature control is implemented in the cooking pan.

²TC indicates temperature controlled flow rate.

The liquid level of tank 2 and the mass flow through the pan is also plotted below.

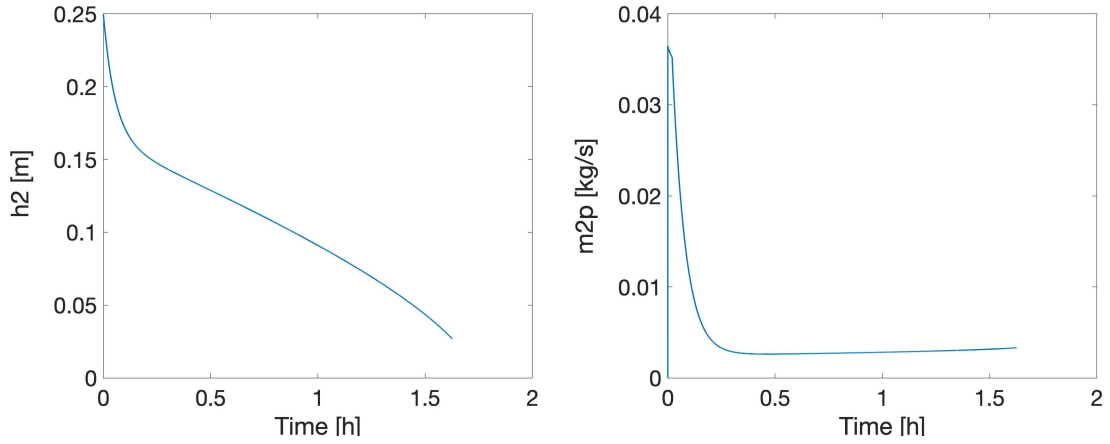


Figure 4.5: Left: Liquid level in tank 2 during the heating and boiling with temperature control. Right: Mass flow rate from tank 2 to the cooking pan during the simulation.

Heat Transfers with Temperature Control

The heat transfers in the system were also plotted in figure 4.6. The plot investigates the delivered power from the cooking pan and identifies the major sources of heat loss. As seen in the figure, the heat transfer to the water, \hat{Q}_{PF} , follows the mass flow rate from tank 2 to the pan.

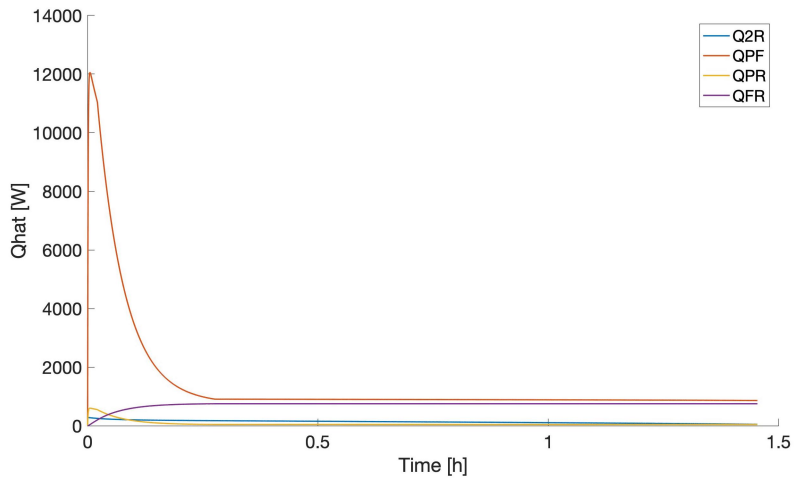


Figure 4.6: Heat transfer values during heating and boiling of the water.

As the water temperature stabilizes at 100 °C, the individual heat transfer streams have smaller variations. Their average values during boiling are reported below in table 4.2. The major heat transfer streams are associated with \hat{Q}_{PF} and heat loss from the cooking pot

surface, \hat{Q}_{FR} . The minor heat losses are associated with heat losses to the room from tank 2, \hat{Q}_{2R} and the pan, \hat{Q}_{PR} .

Table 4.2: Average Heat Transfers at Water Boiling Temperature

Stream	Average Heat Transfer [W]
\hat{Q}_{PF}	891
\hat{Q}_{FR}	753
\hat{Q}_{2R}	118
\hat{Q}_{PR}	45

The time to reach boiling temperature has also been tested experimentally using 2 L of water. Therefore, the case study was simulated with temperature control once more using 2 L of water instead of the initial 10 L. In table 4.3, the average heat transfers and time required to boil are reported for both simulations and the experimental test.³

Table 4.3: Time and Average Heating Output to Reach Water Boiling Temperature

Method	Water Volume [L]	\hat{Q}_{PFavg} [W]	Time to boil [min]
Simulation	10	3725	16.7
Simulation	2	3632	3.4
Experimental	2	3600	3.5

Rice Cooking

With temperature control, the total delivered heat throughout the simulation to the water, $\sum \hat{Q}_{PF}$, is 15.02 MJ. The energy is sufficient to cook two successive batches of rice using 10 L and 6 L of water, respectively. This yields approximately 80 portions of rice. The calculations are derived in appendix B.1.

Cooking Capacity with Lower Load

It might not be necessary to keep the water at boiling temperature throughout the cooking. For cooking rice for instance, a simmering temperature of 82 °C might be sufficient. The possible cooking time for 10 L of water was then extended from 1.18 hours to 2.26 hours, as depicted in figure 4.7 below.

³The experimental value of \hat{Q}_{PFavg} is an estimate, see appendix B.2

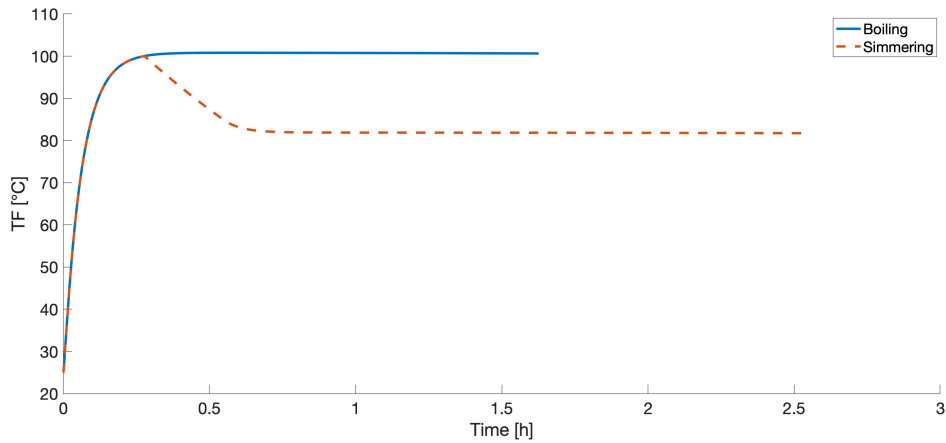


Figure 4.7: Time the system can operate if maintaining a boiling or simmering temperature.

4.3 Case 3: Cooking with Oil Circulation

In case 3, the benefit of circulating the warm oil to extract remaining heat was investigated. The simulation was an extension of case 2 with temperature control. After tank 2 was nearly emptied, oil was circulated in the system, simulated with a constant mass flow rate of 0.001 kg/s between each control volume. As seen in figure 4.8, the boiling temperature is maintained to 2.03 hours after simulation start rather than 1.63 hours without circulation as in case 2. This adds an extra 0.40 hours of cooking time capacity.

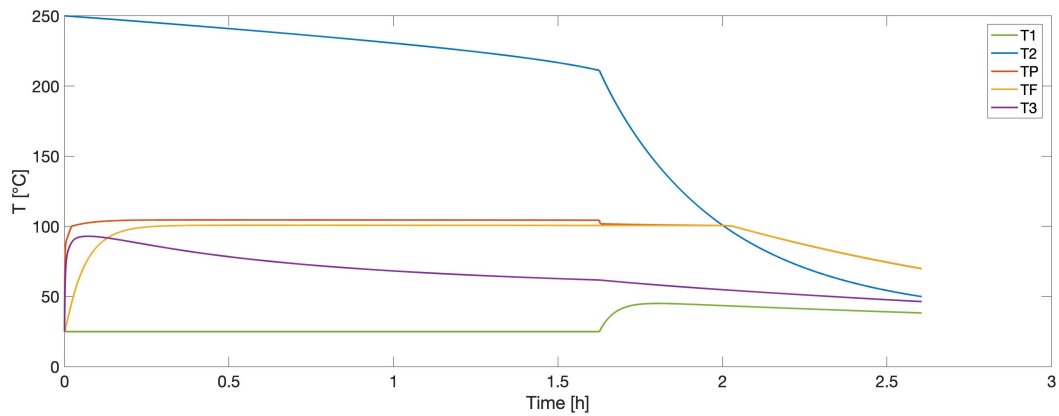


Figure 4.8: Temperature profiles in all control volumes with cooking and recirculation of warm oil.

Figure 4.9 shows the volume fraction in each tank. The initial cooking is simulated until F_2 is 0.05. Then, at 1.63 hours, the fractions stabilize in each tank as a constant mass flow enters and leaves each tank.

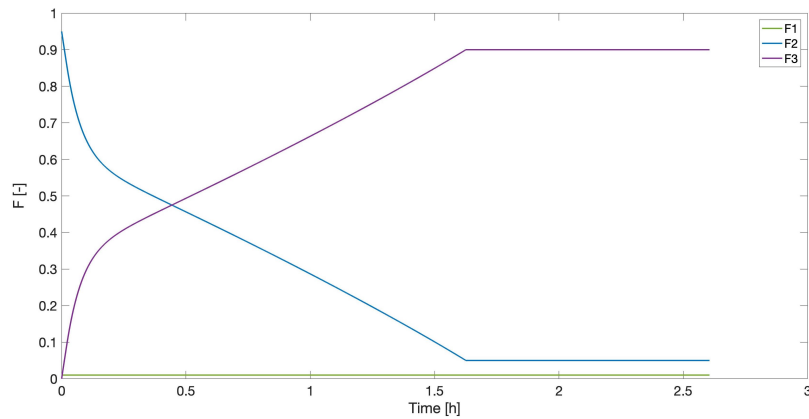


Figure 4.9: Volume fractions in tanks during cooking and circulation of warm oil.

4.4 Case 4: Heat Loss from Tank 2

As the system is to be used for storage of thermal energy, its insulation efficiency is an important characteristic. The temperature change of tank 2 was therefore simulated over 15 hours with an initial temperature of 220 °C. The heat loss was calculated for different volume fractions, where a filled fraction of 0.875 maintained the highest temperature.

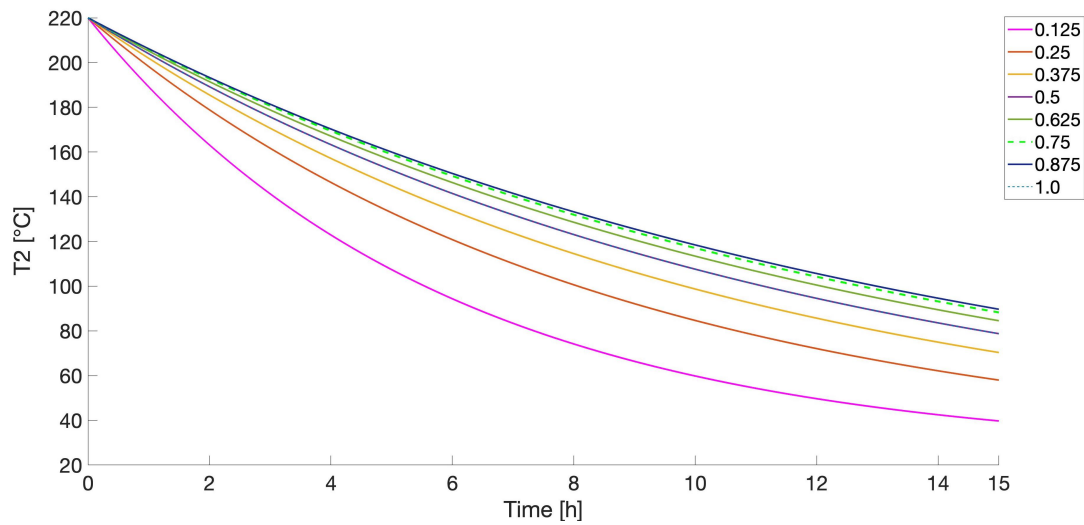


Figure 4.10: Temperature of tank 2 with a varying volume fraction, F_2 . The lines of fractions 1.0 and 0.5 overlap.

5 Discussion

5.1 Method Evaluations

Most of the field tests previously performed have been focused on proof of concept. As a result, caution should be taken to directly compare the model with these tests. Uncertainties in conditions include shifting weather, resulting in variable solar panel effect, wind and ambient temperature. In addition, the flow rate out of tank 2 was manually adjusted in experiments. In the model, thermostat control was implemented for parts of the simulation. Some parameters for the model were estimated based on the experimental data, which introduces uncertainty due to mismatch between experimental and simulation conditions. This will be discussed in detail later.

The numeric integration is done in small time steps to ensure the error to be as small as possible. However, Euler integration is the simplest form of numerical integration, associated with a comparatively large error term compared to other methods. [8] A more sophisticated integration could be implemented, at the cost of longer computational times.

5.2 Discussion of Results

Case Study 1

Figure 4.1 in case study 1 shows that the heating of tank 2 works as expected. The rate of heating slows down somewhat as the temperature increases, resulting in a nonlinear profile. This is due to an increasing heat loss to the environment. The temperature difference between T_2 and T_R increases, which gives a higher heat loss as described in equation 2.33. The heating of 33.9 L oil took 4.03 hours in the simulation versus 5 hours for 30.5 L in the field test. One reason could be a period of lower power supply during the field test due to a short period of cloudy conditions. Another explanation is that the model underestimates heat losses from tank 2.

The temperature control, demonstrated in figure 4.2 also seems to work properly as the temperature maintains between 241.3 and 241.7 °C until the tank is 90% filled. The thermostat is set to open linearly between 200 and 250 °C, where the maximum temperature is never reached. Thus, the thermostatic valve behaves like a proportional controller with a steady state offset error [9].

Case Study 2

Case study 2 indicates that there is significant benefit to controlling the temperature in the cooking pan. By setting the flow rate to a constant 0.01 kg/s, the boiling temperature is

reached at about the same time as with temperature control. However, the total cooking time capacity is less than half because tank 2 empties out quicker. Thus, much energy is wasted by the exaggerated flow. Halving the flow rate to 0.005 kg/s gives a significantly longer cooking time, but also requires a much longer time to reach boiling temperature. Figure 4.4 shows the temperature profiles with temperature control in the pan. As can be seen in figure 4.5, the mass flow is initially high to quickly reach the boiling temperature, but quickly reduced as less additional heat is required to maintain the temperature.

As seen in figure 4.6, the initial heat transfer of \hat{Q}_{PF} seems quite high, delivering approximately 12 kW. In comparison, individual burners on a powerful induction plate are in the range of 4 to 5 kW. [10]. The model likely exaggerates the maximum possible flow rate through the cooking pan, delivering a high maximum heating. This is supported from the data of table 4.3. The time to boil 2 L of water is approximately equal for the field test and the simulation. In the field test, the system is at full flow, while the valve quickly partially closes in the simulation to limit the heat flow.

Figure 4.7 shows the important influence of cooking load on the system's capacity. If the required temperature in the cooking pot is reduced by 18 °C, the cooking time at operating temperature is almost doubled.

Case Study 3

Case study 3 and figure 4.8 shows that a significant amount of heat can be recovered by circulation of the oil. By setting a constant pumping rate for the rest of the system, another 0.40 hours of cooking time was extracted from the system. The conditions of constant and equal mass flow in and out of each control volume is likely unrealistic due to varying levels in each tank. However, the simulation still demonstrates the value of utilizing as much heat as possible, as only manual labor is required to pump the oil back up to tank 1.

Case Study 4

The final case study, illustrated by figure 4.10, indicates that a substantial amount of thermal energy can be stored overnight. Initially, increasing the filling fraction of tank 2 increases the final temperature. The simulations indicate that a filling fraction of 0.875 maintains the highest temperature. As the filling fraction increases further, the oil contact surface area also increases significantly, resulting in larger heat loss.

The equivalent field test left a half filled tank 2 overnight with the temperature sinking from 220 °C to 120 °C. A simulation of the procedure gave a final temperature of 79 °C, which is significantly lower. One explanation could be that the estimated heat loss coefficient

for tank 2, U_2 , is too high. The long duration of the simulation could also propagate a considerable numerical integration error.

5.3 Parameter Estimation

For simplicity, the heat capacity of the oil was assumed constant using the average value in the operating temperature interval. The same assumption was made for the oil density. The two simplifications will mitigate each other to some extent. At low temperatures, the model overestimates the heat required to raise the temperature but underestimates the density and thus effective heat transfer area. For high temperatures, the opposite is true.

Four of the parameters for this model are estimates based on the experimental data and are all related to heat loss. These are the heat transfer coefficient for tank 1 and 3, U , the heat transfer coefficient for tank 2, U_2 , the heat transfer factor from the cooking pot, UA_f , and the heat loss factor for the hot oil in the cooking pan exposed to air, l . The three latter are particularly important in evaluating the cooking capacity of the system. They all describe the loss of thermal energy in control volumes with high temperatures, namely tank 2, the water and the cooking pan.

Sensitivity Analysis

The effect of adjusting U_2 was tested running case study 1a for different values of the heat transfer coefficient. As seen in figure 5.1, the change is nearly linear in the range of 0 to 5 W/m^2K , with a base case value of 2.5. Increasing U_2 outside this range starts giving an exponential-like effect on the required heating time. The analysis indicate that the heat loss transfer coefficient estimate is in a sensible range, with a similar required heating time to field tests. It also indicates that sufficient insulation is important for an efficient system. The heat transfer coefficient for tank 1 and tank 3, U , has not been analyzed to the same extent. This is because tank 2 is designed to be the significant heat storage capacity.

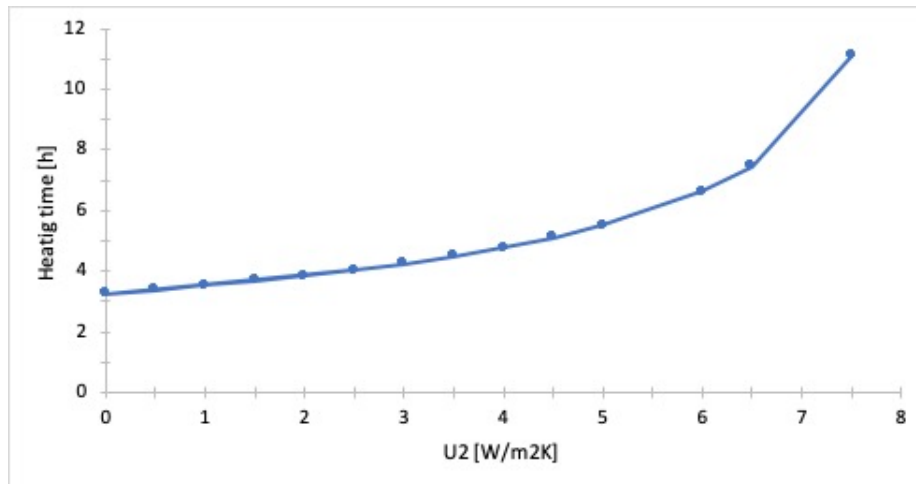


Figure 5.1: Time required to heat a full tank 2 from 66 °C to 250 °C with a varying heat loss coefficient, U_2 .

The heat loss from the casserole to the room is estimated by the heat transfer factor UA_f . In the base case, this value is 10.04 W/K. As seen from figure 5.2, a 20 % increase in the factor gives a much shorter cooking time. This suggests that the heat loss from the casserole is important in determining the cooking time capacity.

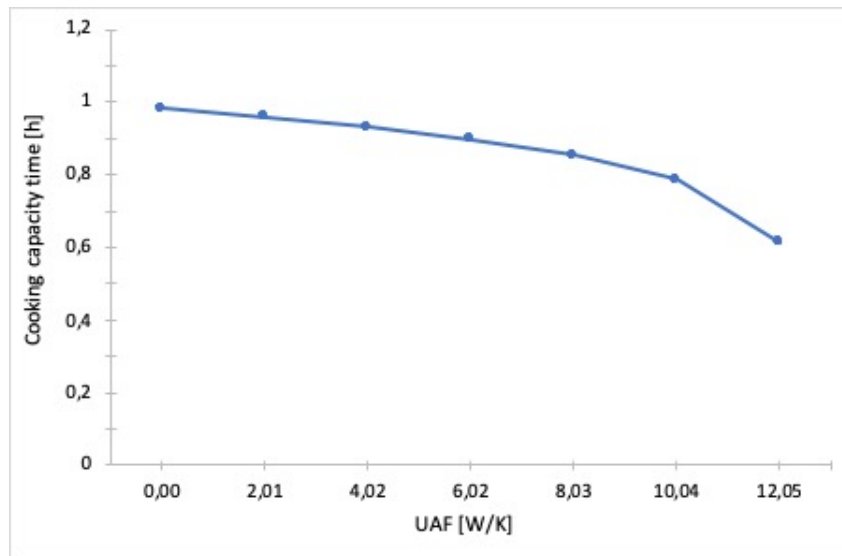


Figure 5.2: Time water is maintained at boiling temperature with varying the heat loss factor for the cooking pot surface, UA_f .

5.4 Field Test Suggestions

In order to estimate the heat transfer parameters with a higher certainty, a couple of additional tests are suggested below.

1. Test of time to heat a full tank 2 on a day without any cloudy periods. This provides a less fluctuating \hat{Q}_{PV} , which gives simpler data for fitting the heat transfer coefficient U .
2. Test of oil mass required to boil water for a given time with or without rice added to the casserole. The experiment provides a basis to account for additional heat required when rice is cooked.

5.5 Further Work

Based on the above discussion, the following further work is recommended

1. Systematic planning and coordination of additional experiments in cooperation with students performing field tests in the spring of 2020.
2. Utilization of new data to perform modifications to heat transfer coefficients and equations to match the new results.
3. Establish and solve an optimization problem for optimal operation of the system.
4. Simulate the effect of adding other renewable energy components to the system such as wind power input.

6 Conclusion

A solar powered thermal energy storage system was modeled in this project. The system consists of three oil tanks which uses heated oil as a heat transfer medium to cook food. The purpose of the model was to demonstrate similar behavior to the physical system and evaluate its cooking capacity. It is also thought to be the starting point for deciding optimal operation strategies.

The model was based on physical principles such as mass and energy balances. Most of the parameters for the simulation were known parameters of the physical system. Several of the parameters used to estimate heat transfers were largely based on experimental data and associated with more uncertainty.

Some of the case studies were designed to match previous field experiments as closely as possible. These studies included time required to heat a full tank, time required to bring water to boiling and the heat loss of a tank of hot oil overnight. Overall, the model matches the trends of the physical system . However, caution must be taken to compare the values directly, as well-defined conditions during the field tests are lacking. Uncertainties in the model are largely associated with the heat transfer coefficients. The sensitivities of these parameters were further investigated for tank 2 and the casserole surface. The estimated heat loss of tank 2 seems to be in a sensible range, requiring a large change to affect model performance significantly. The performance is more sensitive to the estimated heat loss factor from the water through the casserole, UA_f . A 20 % increase in the parameter drastically reduces the available cooking time capacity. Additional field tests could be conducted to obtain more certain estimates of heat transfer parameters.

The system model computes significant cooking capacity for the system. At base case, a full tank of hot oil is able to keep 10 L of water boiling for 1.18 hours with a temperature controlled flow. This corresponds to cooking approximately 80 portions of rice. The system is also rapid, requiring only 3.4 minutes to boil 2 L of water. In addition, tank 2 is able to retain much of its heat overnight, with a final temperature of 90 °C, 15 hours after turning the heating off.

References

- [1] British Petroleum Company, *BP Statistical Review of World Energy*. London: British Petroleum Co., 2019, pp. 2–4.
- [2] P. B. Nielsen, M. Hørmann, J. N. Rud, and F. M. Laugesen, *Renewable energy supply and storage: Guide for planners & developers in sparsely populated areas*. Copenhagen: Nordisk Ministerråd, 2016, p. 39, ISBN: 978-92-893-4805-8.
- [3] S. Ould Amrouche, D. Rekioua, T. Rekioua, and S. Bacha, “Overview of energy storage in renewable energy systems”, *International Journal of Hydrogen Energy*, vol. 41, no. 45, pp. 20 914–20 927, 2016, ISSN: 0360-3199.
- [4] United Nations Economic Commissions for Africa, *2018 Africa Sustainable Development Report: Towards a transformed and resilient continent*. Addis Ababa: United Nations Economic Commissions for Africa, 2018, p. 29.
- [5] S. Thaulé, M. Kolderup, and K. Gustafson, *Excess solar, wind, and hydro power to charge heat storage for cooking*. Trondheim: Norwegian University of Science and Technology, 2019, p. 68.
- [6] S. Skogestad, *Prosessteknikk : masse- og energibalanser*, 2. utg. Trondheim: Tapir, 2003, pp. 218–219, ISBN: 8251918820.
- [7] S. Blundell, *Concepts in Thermal Physics*, 2nd ed. Oxford: Oxford University Press, 2010, pp. 99–101, ISBN: 0-19-157433-3.
- [8] K. E. Atkinson, *Numerical Solution of Ordinary Differential Equations*. Hoboken: Wiley, 2009, pp. 15–16, ISBN: 1-283-33249-3.
- [9] D. E. Seborg, *Process Dynamics and Control*, 3rd ed. Hoboken: Wiley, 2011, pp. 137–138, ISBN: 9780470646106.
- [10] T. Nguyen, “Most Powerful Induction Cooktops (Reviews/Ratings/Prices)”, (*Date Accessed: 07.12.2019*), [Online]. Available: <https://blog.yaleappliance.com/most-powerful-induction-cooktops>.
- [11] M. R. Shulman, “Basic Steamed Long-Grain Rice”, (*Date Accessed: 09.12.2019*), [Online]. Available: <https://cooking.nytimes.com/recipes/1014002-basic-steamed-long-grain-rice>.
- [12] A. Blackman, *Aylward and Findlay’s SI Chemical Data*, 7th ed. Milton: John Wiley & Sons, 2014, p. 176, ISBN: 9780730302469.
- [13] Chempro, “Palm Oil Properties”, (*Date Accessed: 07.11.2019*), [Online]. Available: <https://www.chempro.in/palmoilproperties.htm>.
- [14] Knovel, “Yaws’ Critical Property Data for Chemical Engineers and Chemists - Table 212. Thermal Conductivity - Stainless Steels”, (*Date Accessed: 07.11.2019*), [Online]. Available: https://app.knovel.com/web/view/itable/show.v/rcid:kpYCPDCECD/cid:kt00AAAHWC/viewerType:eptble//root_slug:table-212-

thermal-conductivity---stainless-steels-log-k--a--bt/url_slug:table-212-thermal-conductivity?kpromoter=federation&filter=graph&b-toc-cid=kp.

Appendices

A Additional Case Studies and Plots

A.1 Case 1c: Comparison of Heating Gradually Filling and Filled Tank

It was also investigated whether it would be more efficient to heat up a small amount of oil and gradually fill up the tank, or directly heat a full tank of cold oil. This was performed by running case 1a and 1b a second time, starting at 25 °C and a final filling fraction F_2 of 0.9 in both scenarios. Figure A.1 below shows time required by test one, "filled tank" and test two, "filling tank". Starting with a filled tank took 4.22 hours, while gradual filling took 4.35 hours.

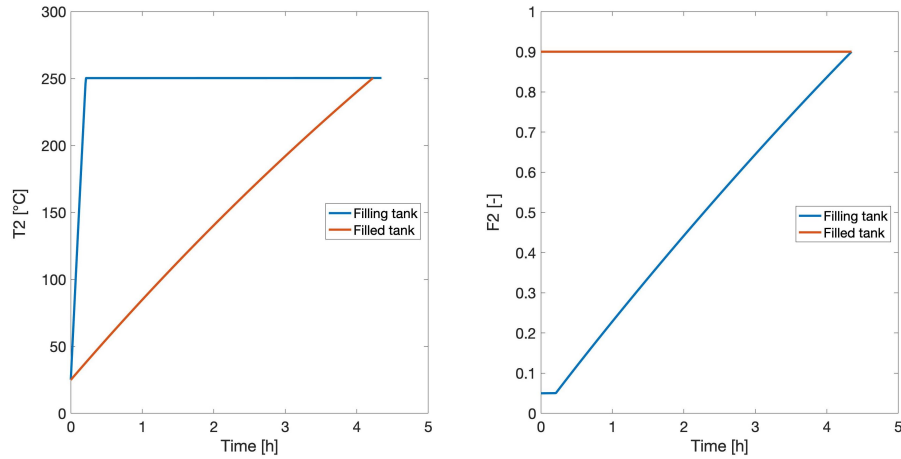


Figure A.1: Left: Comparison of temperature profiles with an initially full or gradually filling tank. Right: Tank 2 volume fractions during the simulation

Figure A.1 suggests that some time can be saved by heating a full tank of cold oil rather than filling a tank gradually. However, the time saved in the test is only about 3 % and likely not of significance.

A.2 Case 2: Constant Hot Oil Flow Rate - Plots

Below are the control volume temperature profiles and tank 2's volume fractions during case 2 with a constant mass flow rate

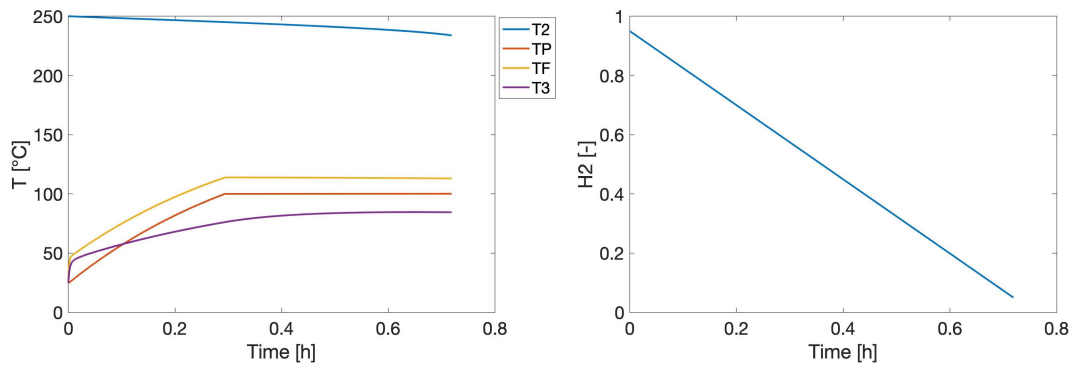


Figure A.2: Left: Temperatures in tank 2, cooking pan, water and tank 3 with a constant mass flow of 0.001 kg/s through the pan. Right: Volume fraction of tank 2 during heating and boiling of water.

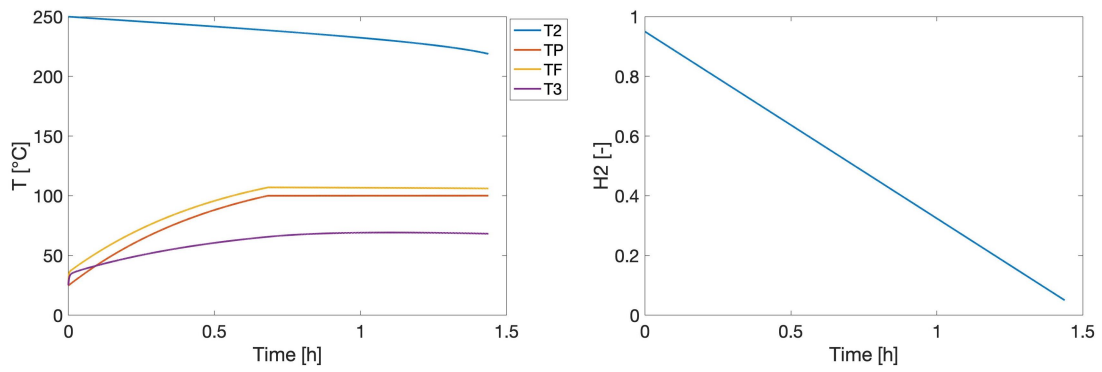


Figure A.3: Left: Temperatures in tank 2, cooking pan, water and tank 3 with a constant mass flow of 0.0005 kg/s through the pan. Right: Volume fraction of tank 2 during heating and boiling of water.

B Hand Calculations

B.1 Rice Cooking Estimations

The total delivered heat energy in case 2 with temperature control, $\sum \hat{Q}_{PF}$, is 15.02 MJ. Bringing a casserole with 10 L water of 25 °C to boil and at boiling point for 20 minutes, $\sum_{t=0}^{t_{boiling}=20} \hat{Q}_{PF}$, required 9.64 MJ. The amount of cooking batch cycles available are

$$Batches = \frac{\sum_{t=0}^t \hat{Q}_{PF}}{\sum_{t=0}^{t_{boiling}=20} \hat{Q}_{PF}} = \frac{15.02MJ}{9.64MJ} = 1.6 \quad (B.1)$$

The calculation assumes that a separate casserole initially at room temperature is used for each batch. The result is equivalent to a full batch of 10 L water and another batch of 6 L water. Assuming one portion of rice is 1 dL and a typical water to rice ratio of 2:1[11], the amount of rice portions are

$$Portions = \frac{16L}{0.2L/portion} = 80 \quad (B.2)$$

B.2 Case 2: Average Experimental Heat Transfer

In the thesis by Thaulé et.al., the time to heat 2 L of water to boiling was 3.5 minutes. In comparison, the time to heat 2 L of water using a 1800 W water boiler took 7 minutes. Assuming the heat losses from the water boiler and the cooking pot are similar, this indicates the average heat transfer from the cooking pan to pot, \hat{Q}_{PF} , was approximately 3600 W.

C MATLAB Codes

Below are samples of the MATLAB codes used for the various case studies.

C.1 Case 1a Simulation

```
1 %% CASE STUDY 1a: Heating full storage tank
2
3 clear all
4
5 %% Constant parameters
6 eps=0.00000001; %small number to avoid division by zero
7 AThermostatHole = pi*0.005^2/4; %area of fully open thermostat [m2]
8 g=9.8; %[m/s2]
9 Dtank= 0.2765; %tank diameter [m]
10 Ltank=0.57; %tank length [m]
11 h12 = 0.45; %height pipe between 1 and 2 [m]
12 h23 = 0.75; %height pipe between 2 and 3 [m]
13 Atank = pi*Dtank^2/4; %tank end area [m]
14 Vtank = Atank*Ltank; %Volume of tank [m3]
15 rho=840; %avg density 20–250C [kg/m3]
16 c=2242; %avg heat capacity oil 20–250C, [J/kgK]
17 cpw = 4200; %heat capacity water [J/kgK]
18 Hvapw = 2257*1000; %Enthalpy of vaporization water [J/kg]
19 Ct = 0.5; %discharge coefficient thermostat [-]
20 Cv = 1; %discharge coefficient valve [-]
21 d=0.015; %pipe diameter [m]
22 a=pi*d^2/4; %pipe area [m]
23 Av1 = a; %valve opening, same as pipe area [m2]
24 l = 0.05; %fraction heat loss to environment [-]
25 k = 16.3; %steel thermal conduction coefficient [W/mK]
26 dx = 0.005; %casserole thickness [m]
27 h = (k/dx); %heat transfer coefficient [W/m2K]
28 U = 2.5; %tank heat transfer coefficient [W/m2K]
29 f = 10; %non-insulation factor [-]
30 Ap = pi*0.14^2; %Plate heat transfer area [m2]
31 UAF = 0.05*h*Ap; %heat transfer coefficient for loss pan to air [W/K]
32 QPVtid=0; %simulation time vector [s]
33 t=0; %simulation time [s]
34 m12=0; m2p=0; m31=0; %initialization mass flows [kg/s]
35
36 %% Variable parameters
37 dt=0.5; %integration step [s]
38 T1=273+25; T2=273+66; T3=T1; To=T1; TP = T1; TF = T1; %starting ...
```

```

        temperatures [K]
39 QPV=1000; %panel effect [W]
40 Ftank=0.99; %filled volume fraction of tank [-]
41 At = eps; % Thermostat hole closed to start [m2]
42 Pump = 0; %pump from 3 to 1 [kg/s]
43 Tstart = 273+ 200; %opening temperature thermostat hole [K]
44 Tstop = 273 + 250; %fully open thermostat [K]
45 F1=0; % volume fractions
46 F2=Ftank;
47 F3=0;
48 M1=rho*Vtank*F1; %control volume mass [kg]
49 M2=rho*Vtank*F2;
50 MP = 0.5;
51 MF = 10;
52 M3=0;
53
54 %% Simulation
55 [h1, A1] = PerimeterHeight(F1,Dtank, Ltank); % level heights [m] and heat ...
        transfer area [m2]
56 [h2, A2] = PerimeterHeight(F2,Dtank, Ltank);
57 [h3, A3] = PerimeterHeight(F3,Dtank, Ltank);
58
59
60 M1Old=M1; M2Old=M2; M3Old=M3; MPold=MP; MFold=MF;
61 T1Old=T1; T2Old=T2; T3Old=T3; TPold=TP; TFold=TF;
62
63 T1Plot=T1; T2Plot=T2; T3Plot=T3; TPPlot=TP; TFPlot=TF;
64
65 I = 1;
66
67 while T2 < 250+273
68     t=t+dt; % increment time
69
70 M1Old=M1; M2Old=M2; M3Old=M3; MPold=MP; MFold=MF; %set old values
71 T1Old=T1; T2Old=T2; T3Old=T3; TPold=TP; TFold=TF;
72
73 [h1, A1] = PerimeterHeight(F1,Dtank, Ltank); % get surface for heat
74 [h2, A2] = PerimeterHeight(F2,Dtank, Ltank); % transfer and oil height
75 [h3, A3] = PerimeterHeight(F3,Dtank, Ltank);
76
77 % New flows
78 m12 = 0;
79
80 m2p = 0;
81
82 m31 = Pump;

```



```

83
84 % new masses
85 M1 = M1Old + dt*(m31-m12);
86 M2 = M2Old + dt*(m12-m2p);
87 M3 = M3Old + dt*(m2p-m31);
88 MP = MP0ld + dt*(m2p-m2p);
89 MF = MF0ld;
90
91 % volume fractions
92 F1=M1/(rho*Vtank);
93 F2=M2/(rho*Vtank);
94 F3=M3/(rho*Vtank);
95
96 % new temperatures
97 dT1 = (m31*(T3Old-T1Old)-f*U*A1*(T1Old-To)/c)/(M1+eps);
98 T1 = T1Old + dT1*dt;
99
100 dT2 = (m12*(T1Old-T2Old)-U*A2*(T2Old-To)/c+QPv/c)/(M2+eps);
101 T2 = T2Old + dT2*dt;
102
103 dTP = (m2p*(T2Old-TP0ld)-(1+1)*(h*Ap*(TP0ld-TF0ld))/c)/(MP+eps);
104 TP = TP0ld + dTP*dt;
105
106 if (TF > 100+273 && TP > TF) %additional heat at water boiling point ...
    gives vaporization
107 enth = Hvapw;
108 else
109     enth = cpw;
110 end
111
112 dTF = ((h*Ap*(TP0ld-TF0ld)-UAF*(TF0ld-To))/enth)/(MF+eps);
113 TF = TF0ld + dTF*dt;
114
115 dT3 = (m2p*(T2Old-T3Old)-f*U*A3*(T3Old-To)/c)/(M3+eps);
116 T3 = T3Old + dT3*dt;
117
118 T1Plot(I)=T1-273;
119 T2Plot(I)=T2-273;
120 T3Plot(I)=T3-273;
121 TFPlot(I) = TF-273;
122 TPPlot(I) = TP-273;
123 h1Plot(I)=h1; h2Plot(I)=h2; h3Plot(I)=h3;
124 m12Plot(I)=m12; m2pPlot(I)=m2p; m31Plot(I)=m31;
125 AtPlot(I)=At;
126 tid(I)=t;
127 tidPlot = tid/3600;

```

```

128
129 I = I+1;
130 end
131
132 size = I-1;
133 QPVPlot = ones(1,size*2);
134 QPVtid = ones(1,size*2);
135 for i = 1:I
136     QPVPlot(i) = 0;
137     QPVtid(i) = (-I+i)/7200;
138 end
139 for i = I+1:2*I
140     QPVPlot(i) = 1000;
141     QPVtid(i) = (-I+i)/7200;
142 end
143
144 %Plot of temperature 2 and the solar input QPV
145 subplot(1,2,1)
146 plot(tidPlot,T2Plot,'LineWidth',1.5);
147 ylabel('T2 [C]');
148 xlabel('Time [h]');
149 set(gca,'FontSize',20)
150
151 subplot(1,2,2)
152 stairs(QPVtid,QPVPlot,'LineWidth',1.5);
153 ylabel('QPV [W]');
154 xlabel('Time [h]');
155 set(gca,'FontSize',20)

```

C.2 Liquid Level and Heat Transfer Area Calculation

```

1 function [ height, area ] = PerimeterHeight( Farg, Darg, Larg )
2 % compute perimeter and height for given volume fraction
3 Atank= (pi*Darg^2)/4;
4 fcn = @(theta) theta-sin(theta)-2*pi*Farg;
5 theta = fzero(fcn,1);
6 height = (1-cos(theta/2))*Darg/2;
7 perimeter = theta*Darg/2;
8 area=Larg*perimeter + Atank*Farg*2;
9
10 end

```

C.3 Case 2: Cooking with Temperature Control Simulation

```
1 %% CASE STUDY 2: Cooking with heated oil – temperature control
2 clear all
3 %% Constant parameters
4 eps=0.00000001; %small number to avoid division by zero
5 AThermostatHole = pi*0.005^2/4; %area of fully open thermostat [m2]
6 g=9.8; %[m/s2]
7 Dtank= 0.2765; %tank diameter [m]
8 Ltank=0.57; %tank length [m]
9 h12 = 0.45; %height pipe between 1 and 2 [m]
10 h23 = 0.75; %height pipe between 2 and 3 [m]
11 Atank = pi*Dtank^2/4; %tank end area [m]
12 Vtank = Atank*Ltank; %Volume of tank [m3]
13 rho=840; %avg density 20–250C [kg/m3]
14 c=2242; %avg heat capacity oil 20–250C, [J/kgK]
15 cpw = 4200; %heat capacity water [J/kgK]
16 Hvapw = 2257*1000; %Enthalpy of vaporization water [J/kg]
17 Ct = 0.5; %discharge coefficient thermostat [-]
18 Cv = 1; %discharge coefficient valve [-]
19 d=0.015; %pipe diameter [m]
20 a=pi*d^2/4; %pipe area [m]
21 Av1 = a; %valve opening, same as pipe area [m2]
22 l = 0.05; %fraction heat loss to environment [-]
23 k = 16.3; %steel thermal conduction coefficient [W/mK]
24 dx = 0.005; %casserole thickness [m]
25 h = (k/dx); %overall heat transfer coefficient [W/m2K]
26 U = 2.5; %tank heat transfer coefficient [W/m2K]
27 f = 10; %non-insulation factor [-]
28 Ap = pi*0.14^2; %Plate heat transfer area [m2]
29 UAF = 0.05*h*Ap; %heat transfer coefficient for loss pan to air [W/K]
30 tid=0; %simulation time vector [s]
31 t=0; %simulation time [s]
32 m12=0; m2p=0; m31=0; %initialization mass flows [kg/s]
33
34 %% Variable parameters
35 dt=0.5; %integration step [s]
36 T1=273+25; T2=273+250; T3=T1; To=T1; TP = T1; TF = T1; %starting ...
    temperatures [K]
37 QPV=0; %panel effect [W]
38 Ftank=0.95; %filled volume fraction of tank [-]
39 At = eps; % Thermostat hole closed to start [m2]
40 Pump = 0; %pump from 3 to 1 [kg/s]
41 Tstart = 273+ 100; %opening temperature thermostat hole [K]
```

```

42 Tstop = 273 + 105; %fully open thermostat [K]
43 F1=0; % volume fractions
44 F2=Ftank;
45 F3=0;
46 M1=rho*Vtank*F1; %control volume mass [kg]
47 M2=rho*Vtank*F2;
48 MP = 0.5;
49 MF = 10;
50 M3=0;
51
52 %% Simulation
53 [h1, A1] = PerimeterHeight(F1,Dtank, Ltank); % level heights [m] and heat ...
      transfer area [m2]
54 [h2, A2] = PerimeterHeight(F2,Dtank, Ltank);
55 [h3, A3] = PerimeterHeight(F3,Dtank, Ltank);
56
57 M1Old=M1; M2Old=M2; M3Old=M3; MPold=MP; MFold=MF;
58 T1Old=T1; T2Old=T2; T3Old=T3; TPold=TP; TFold=TF;
59
60 T1Plot=T1; T2Plot=T2; T3Plot=T3; TPPlot=TP; TFPlot=TF;
61
62 I = 1;
63
64 while F2 > 0.05
65     t=t+dt; % increment time
66
67 M1Old=M1; M2Old=M2; M3Old=M3; MPold=MP; MFold=MF; %set old values
68 T1Old=T1; T2Old=T2; T3Old=T3; TPold=TP; TFold=TF;
69
70 [h1, A1] = PerimeterHeight(F1,Dtank, Ltank); % get surface for heat
71 [h2, A2] = PerimeterHeight(F2,Dtank, Ltank); % transfer and oil height
72 [h3, A3] = PerimeterHeight(F3,Dtank, Ltank);
73
74 % New flows
75 m12 = 0;
76
77 Ftot2 = (1/(Ct*At))^2 + (1/(Cv*Av1))^2;
78 Htot2 = h23 + h2 - h3;
79 m2p = rho*sqrt(2*g*Htot2/Ftot2);
80
81 m31 = Pump;
82
83 % new masses
84 M1 = M1Old + dt*(m31-m12);
85 M2 = M2Old + dt*(m12-m2p);
86 M3 = M3Old + dt*(m2p-m31);

```

```

87 MP = MPold;
88 MF = MFold;
89
90 % volume fractions
91 F1=M1/(rho*Vtank);
92 F2=M2/(rho*Vtank);
93 F3=M3/(rho*Vtank);
94
95 % new temperatures
96 dT1 = (m31*(T3old-T1old)-f*U*A1*(T1old-To)/c)/(M1+eps);
97 T1 = T1old + dT1*dt;
98
99 dT2 = (m12*(T1old-T2old)-U*A2*(T2old-To)/c+QPv/c)/(M2+eps);
100 T2 = T2old + dT2*dt;
101 Q2R = U*A2*(T2old-To);
102
103 dTP = (m2p*(T2old-TPold)-(1+l)*(h*Ap*(TPold-TFold))/c)/(MP+eps); %!% heat ...
      loss to environment
104 TP = TPold + dTP*dt;
105 QPF = h*Ap*(TPold-TFold);
106 QPR = l*QPF;
107
108 if (TF > 100+273 && TP > TF)
109     enth = Hvapw;
110 else
111     enth = cpw;
112 end
113
114 dTF = ((h*Ap*(TPold-TFold)-UAF*(TFold-To))/enth)/(MF+eps);
115 TF = TFold + dTF*dt;
116 QFR = UAF*(TFold-To);
117
118 dT3 = (m2p*(TPold-T3old)-f*U*A3*(T3old-To)/c)/(M3+eps);
119 T3 = T3old + dT3*dt;
120
121 % new thermostat opening 2, linear
122 OpeningFraction = 1-(TP-Tstart)/(Tstop-Tstart);
123 if (OpeningFraction<0) OpeningFraction=0; end; % limit to closed
124 if (OpeningFraction>1) OpeningFraction=1; end; % limit to fully open
125 At = OpeningFraction*AThermostatHole + eps;
126
127 T1Plot(I)=T1-273;
128 T2Plot(I)=T2-273;
129 T3Plot(I)=T3-273;
130 TFPlot(I) = TF-273;
131 TPPlot(I) = TP-273;

```

```

132 h1Plot(I)=h1; h2Plot(I)=h2; h3Plot(I)=h3;
133 m12Plot(I)=m12; m2pPlot(I)=m2p; m31Plot(I)=m31;
134 AtPlot(I)=At;
135 tid(I)=t;
136 F2Plot(I) = F2;
137 Q2RPlot(I) = Q2R;
138 QPFPlot(I) = QPF;
139 QPRPlot(I) = QPR;
140 QFRPlot(I) = QFR;
141 tidPlot = tid/3600;
142 I = I+1;
143 end
144
145 hold on
146 plot(tidPlot,T2Plot,'LineWidth',2)
147 plot(tidPlot,TPPlot,'LineWidth',2)
148 plot(tidPlot,TFPlot,'LineWidth',2)
149 plot(tidPlot,T3Plot,'LineWidth',2)
150 ylabel('T [C]');
151 xlabel('Time [h]');
152 set(gca,'FontSize',20)
153 legend('T2','TP','TF','T3')
154
155 %Plot of temperature 2 and the mass flow rate m12
156 % subplot(1,2,1)
157 % plot(tidPlot,h2Plot,'LineWidth',1.5);
158 % ylabel('h2 [m]');
159 % xlabel('Time [h]');
160 % set(gca,'FontSize',20)
161 %
162 % subplot(1,2,2)
163 % plot(tidPlot,m2pPlot,'LineWidth',1.5);
164 % ylabel('m2p [kg/s]');
165 % xlabel('Time [h]');
166 % set(gca,'FontSize',20)
167
168 %Plot of heat transfer streams
169 % hold on
170 % plot(tid/3600,Q2RPlot,'LineWidth',1.5)
171 % plot(tid/3600,QPFPlot,'LineWidth',1.5)
172 % plot(tid/3600,QPRPlot,'LineWidth',1.5)
173 % plot(tid/3600,QFRPlot,'LineWidth',1.5)
174 % ylabel('Qhat [W]');
175 % xlabel('Time [h]');
176 % set(gca,'FontSize',20)
177 % legend('Q2R','QPF','QPR','QFR')

```

D Simulation Parameters

All parameters with a reference to the system are parameters taken from the system in Arusha or at the NTNU laboratory. Other references are retrieved from literature, with the exception of items marked "estimate". These are the uncertain parameters, considered further in the discussion section. The parameters \hat{Q}_{PV} and \hat{m}_{pump} are reported as ranges because they vary between case studies. The parameter nomenclature in table D.1 matches the symbols used in the report and therefore vary from the MATLAB scripts.

Table D.1: Parameters Used in MATLAB Simulations

Parameter	Description	Value Range	Unit	Reference
\hat{Q}_{PV}	Solar powered heating input	0-1000	W	System
AthermoStatHole	Cross-sectional area of thermostat	1.963e-5	m^2	System
g	Acceleration of gravity	9.8	m/s^2	[12]
r	Tank radius	0.138	m	System
L	Tank length	0.570	m	System
h_{12}	Pipe height difference tank 1 to 2	0.450	m	System
h_{23}	Pipe height difference tank 2 to 3	0.750	m	System
A	Tank end area	0.060	m^2	System
V	Full tank volume	34.226	dm^3	System
ρ	Density of oil	840	kg/m^3	[13]
Cp_{oil}	Heat capacity of oil	2242	J/kgK	[13]
Cp_{water}	Heat capacity water	4200	J/kgK	[12]
C_t	Thermostat discharge coefficient	0.5	-	System
C_v	Manual valve discharge coefficient	1	-	System
d	Pipe diameter	0.015	m	System
a	Pipe area	1.767e-4	m^2	System
A_v	Cross-sectional area of manual valve	1.767e-4	m^2	Estimate
l	Fraction heat loss to environment	0.05	-	Estimate
k	Steel thermal conductivity	16.3	W/mK	[14]
dx	Casserole bottom thickness	0.005	m	System
h_{PF}	Heat transfer coefficient casserole	3260	W/m^2K	-
U	Heat transfer coefficient tank 2	2.5	W/m^2K	Estimate
f	Non-insulated tanks loss factor	10	-	Estimate
A_p	Area casserole bottom	0.0616	m^2	System
\hat{m}_{pump}	Massflow pumped tank 3 to 1	0-0.01	kg/s	System

The justification for estimating the heat transfer coefficients U and U_2 by the experimental data is that they are highly dependent on the amount of insulation on the tanks. With structured experiments and a finalized design of the physical system, these coefficients can be determined with higher certainty.

The data of field test equivalent to case 1a and 4 were used to estimate U_2 . Both tests are associated with uncertain field conditions. The time to heat a full storage tank has input power, ambient temperature and oil densities as major variables. Estimating the coefficient

based on the heat loss overnight include uncertainties such as limiting heat transfer at daytime by solar radiation, variable wind and ambient temperature conditions.